11-13-2017

Late Quaternary uplift along the North America-Caribbean plate boundary: Evidence from the sea level record of Guantanamo Bay, Cuba

Daniel R. Muhs

Eugene S. Schweig

Kathleen R. Simmons

Robert B. Halley

Quaternary Science Reviews 178 (2017) 54–76

Contents lists available at ScienceDirect

Quaternary Science Reviews

journal homepage: www.elsevier.com/locate/quascirev

Late Quaternary uplift along the North America-Caribbean plate boundary: Evidence from the sea level record of Guantanamo Bay, Cuba

Daniel R. Muhs*, Eugene S. Schweig, Kathleen R. Simmons, Robert B. Halley

U.S. Geological Survey, MS 980, Box 25046, Federal Center, Denver, CO 80225, USA

ARTICLE INFO

Article history:
Received 5 January 2017
Received in revised form
13 October 2017
Accepted 17 October 2017
Available online 13 November 2017

Keywords:
Pleistocene
Sea level changes
North Atlantic
U-Th series
Geomorphology
Coastal
Cuba
Uplift

ABSTRACT

The tectonic setting of the North America-Caribbean plate boundary has been studied intensively, but some aspects are still poorly understood, particularly along the Oriente fault zone. Guantanamo Bay, southern Cuba, is considered to be on a coastline that is under a transpressive tectonic regime along this zone, and is hypothesized to have a low uplift rate. We tested this by studying emergent reef terrace deposits around the bay. Reef elevations in the protected, inner part of the bay are ~11–12 m and outer-coast, wave-cut benches are as high as ~14 m. Uranium-series analyses of corals yield ages ranging from ~133 ka to ~119 ka, correlating this reef to the peak of the last interglacial period, marine isotope stage (MIS) 5.5. Assuming a span of possible paleo-sea levels at the time of the last interglacial period yields long-term tectonic uplift rates of 0.02–0.11 m/ka, supporting the hypothesis that the tectonic uplift rate is low. Nevertheless, on the eastern and southern coasts of Cuba, east and west of Guantanamo Bay, there are flights of multiple marine terraces, at higher elevations, that could record a higher rate of uplift, implying that Guantanamo Bay may be anomalous. Southern Cuba is considered to have experienced a measurable but modest effect from glacial isostatic adjustment (GIA) processes. Thus, with a low uplift rate, Guantanamo Bay should show no evidence of emergent marine terraces dating to the ~100 ka (MIS 5.3) or ~80 ka (MIS 5.1) sea stands and results of the present study support this.

Published by Elsevier Ltd.

1. Introduction

The complex boundary between the North America plate and the Caribbean plate at its northern margin (Fig. 1) is considered to be primarily a left-lateral, strike-slip zone, ~100–~250 km wide, that extends over a distance of ~2000 km (Fig. 1). East of the spreading zone near the Cayman Islands, the plate boundary is dominated by two main subparallel faults, the Enriquillo-Plantain Garden fault zone (often called the "EPGFZ") in the south and the Oriente-Septentrional fault zone in the north (Fig. 2; note that just the Oriente portion of the Oriente-Septentrional fault zone is shown here). The North America-Caribbean plate boundary is seismically active and has been studied intensively (Calais et al., 1998; Mann, 2007; Mann et al., 1995, 2002; Pindell and Kennan, 2009; Prentice et al., 2010). Mann et al. (2002), using Global Positioning System (GPS) measurements, infer that the rigid interior of the Caribbean plate is moving northeastward, but rates of horizontal movement vary among individual crustal blocks within the plate, ranging from 19 to 20 mm/yr (e.g., Puerto Rico) to 4–17 mm/yr (e.g., Dominican Republic). Although much of the movement along the northern plate boundary is known to be horizontal, detailed studies have shown that vertical movement is also a component of Quaternary tectonics, and late Quaternary uplift rates vary significantly along its length. For example, Mann et al. (1995), studying the emergent, ~120 ka coral reef terraces in Haiti, report that uplift rates vary from ~0.37 m/ka in the northwestern peninsula, to ~0.19 m/ka in the western part of Haiti, to zero in the south-central part of western Haiti, on Gonave Island. Higher uplift rates in some areas may be due to restraining bends in the major strike-slip faults that accommodate movement along the North America-Caribbean plate boundary (Mann, 2007).

To the west of Haiti, movement along the North America-Caribbean plate boundary is accommodated primarily by the Oriente fault zone, which parallels the southern coast of Cuba (Fig. 2). Rojas-Agramonte et al. (2005) proposed that the Oriente fault zone has undergone considerable evolution over time, from a region

* Corresponding author.
E-mail address: dmuhs@usgs.gov (D.R. Muhs).

https://doi.org/10.1016/j.quascirev.2017.10.024
0277-3791/Published by Elsevier Ltd.

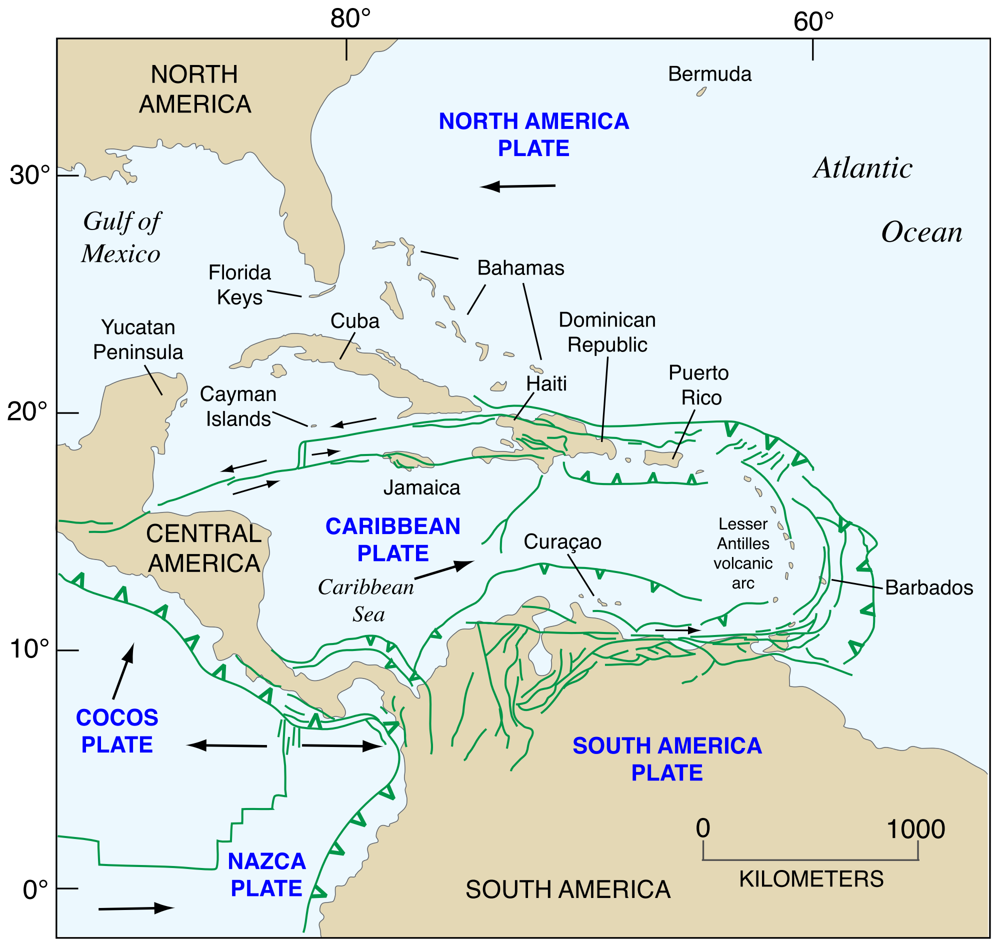

Fig. 1. Tectonic map of the Caribbean Basin and surrounding areas, showing faults (redrawn from Mann (2007) and Pindell and Kennan (2009)), lithospheric plates, directions of present plate movements (arrows), and localities referred to in text.

dominated by compression (late Eocene-Oligocene), to transtension (late Oligocene to Miocene [?]), to transpression (Pliocene to present), when the region had fully evolved into a transform fault zone. If the Oriente fault zone is now characterized by transpression, there should be a measurable component of vertical movement, although possibly small. Such a vertical component of movement could be expressed as uplifted, wave-cut marine terraces or uplifted, constructional coral reef terraces, similar to what Mann et al. (1995) report for Haiti.

Going back more than a century, early investigators noted the presence of emergent coral reef terraces on the coasts of Cuba, but struggled with interpretations of whether these landforms represented uplift, subsidence, or both (Agassiz, 1894; Crosby, 1882; Hill, 1895; Vaughn, 1919). Part of the frustration for these pioneering scientists in interpreting the Cuban terraces was likely due to Darwin's (1889, with earlier editions in 1842 and 1874) theory of coral reef formation, which posits that coral reefs form as a result of long-term regional subsidence. Thus, the presence of *emergent* coral reef terraces on the coast of Cuba, sometimes at considerable elevation, was difficult for early investigators to reconcile with long-term subsidence.

Later investigators provided new hypotheses about the terraces of southern Cuba. Taber (1934) studied a flight of 12 terraces situated ~22 km to the east of Cabo Cruz (Fig. 2). He considered that the terraces in southern Cuba were erosional, wave-cut features, rather than constructional reef terraces, but he recognized that the highest of these terraces (at least ~300 m above present sea level) were too high to be explained by eustatic sea-level rise from any Pleistocene interglacial period. Thus, he concluded that there must have been Quaternary uplift and in fact offered the possibility that the lowest terrace in southern Cuba could even be of Holocene age, implying a relatively high rate of uplift. Taber (1934) inferred that each terrace represented a discrete, presumably coseismic, uplift event. A few decades later, Horsfield (1975), in a pan-Caribbean review of marine terrace records, also noted that a detailed marine terrace record is present along the southern coast of Cuba. Consistent with modern concepts of marine terraces and sea level history, however, he recognized that each terrace likely represented an interglacial high-sea stand, rather than a discrete coseismic event. Horsfield (1975) hypothesized that the numbers of terraces and the altitudes of the highest terrace were positively correlated with uplift rate. Thus, by these criteria, Horsfield (1975) inferred that along the eastern Cuban coast, uplift rates would be highest near Punta de Maisí (Fig. 2), where his estimates of the number of terraces was greatest and terrace elevations are highest. He speculated that uplift rates should decrease to the west, toward Cabo Cruz. More recently, Rojas-Agramonte et al. (2005) reported marine terraces at elevations up to ~200 m in the Santiago area of southern Cuba (Fig. 2), and inferred that these landforms must have been elevated by tectonic uplift. Because of the relatively high elevations of some of the terraces in this part of Cuba, Rojas-Agramonte et al. (2005, p. 177) interpreted the southeastern part of the island to be experiencing a high rate of tectonic uplift.

It is important to point out, however, that in the absence of

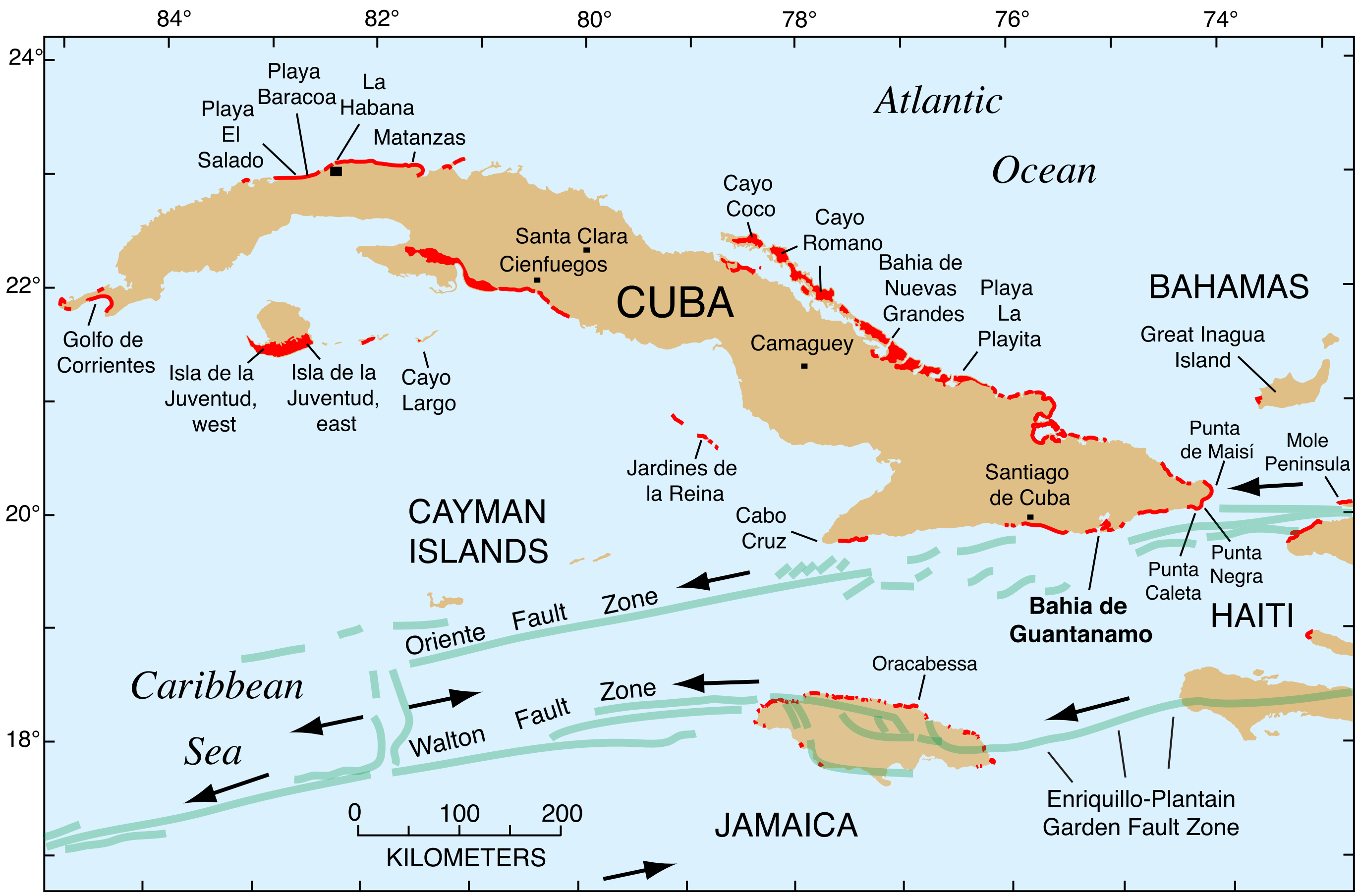

Fig. 2. Map of Cuba, adjacent islands, and active faults near the southeastern part of the island (from Mann, 2007). Red areas in Cuba show extent of the Jaimanitas Formation, an emergent coral reef limestone (compiled by the present authors from data in Academia de Ciencias de Cuba, 1988); red areas shown on other islands are emergent coral reef terraces dating to, or thought to date to, the last interglacial period (compiled from Henry, 1978a, 1978b; Chen et al., 1991; and Mann et al., 1995). (For interpretation of the references to colour in this figure legend, the reader is referred to the web version of this article.)

terrace ages, numbers of terraces and their elevations are not necessarily reliable indicators of uplift rates. For example, the northwest coast of Haiti and the Huon Peninsula of New Guinea both host about 20 uplifted reef terraces, but their uplift rates, based on the age and elevation of the ~120,000-yr-old terrace, differ by as much as a factor of seven (Bloom et al., 1974; Dodge et al., 1983). Part of the explanation for the difference between the geomorphic record of Haiti and New Guinea may be related to the potential for preservation. On New Guinea, older terraces, perhaps of the same age as the highest ones on Haiti, may once have existed, but with higher rainfall, erosional removal of old landforms is much more likely. Along coastlines with similar climates, where preservation potential might be approximately equal, greater numbers of terraces and terraces at higher elevations likely do have some tectonic significance, as hypothesized by Horsfield (1975).

Regional-scale mapping by Cuban geologists (Academia de Ciencias de Cuba, 1988) indicates that the lowest-elevation marine terrace of Cuba could be broadly of the same age along its length and is a constructional coral reef terrace, rather than an erosional landform. The limestone of which this terrace is composed is referred to as the Jaimanitas Formation (Cabrera and Peñalver, 2001; Portell et al., 2008, 2009; Rojas-Agramonte et al., 2005; Toscano et al., 1999). This formation is widespread around much of the coastline of Cuba (Fig. 2). In the Havana (La Habana) area (Fig. 2), Toscano et al. (1999) reported three U-series ages of corals that indicate that at least in this part of Cuba, the Jaimanitas Formation could date to the last interglacial period, ~120 ka. The Jaimanitas Formation in the Havana area is only 1 m–3 m above sea level (Toscano et al., 1999). Rojas-Agramonte et al. (2005) mapped the formation along reaches of the southern Cuban coast east and west of Santiago. Specifically in the Guantanamo Bay area of southern Cuba, Meinzer (1933) did a remarkable job of mapping what is now recognized as the Jaimanitas Formation, done without the aid of aerial photographs, and conducting his field studies on horseback in 1915.

Herein, we report results of new studies of the emergent coral reef record at Guantanamo Bay, with field mapping, stratigraphy, differential GPS elevation measurements, and ages of corals using uranium-series geochronology. These data, along with considerations of the Quaternary sea level record, allow determination of late Quaternary uplift rates. Specifically, we test the hypothesis that the southern coast of Cuba could be experiencing at least modest late Quaternary uplift due to a transpressional tectonic regime, using ages and elevations of an emergent coral reef terrace.

In addition, we wish to examine the coral reef record at Guantanamo Bay in order to test whether what is mapped as the Jaimanitas Formation in this part of Cuba dates to ~120 ka, as in the Havana area. The last interglacial period, identified as marine isotope stage (MIS) 5.5 or 5e in the deep-sea, foraminiferal, oxygenisotope record (Martinson et al., 1987), is of considerable interest as a possible analog for a future warmer Earth (Otto-Bliesner et al., 2006; Overpeck et al., 2006; Clark and Huybers, 2009; Murray-Wallace and Woodroffe, 2014). There are, however, a number of interesting questions about this interglacial period, particularly with regard to its sea level history. Both modeling efforts (Kopp et al., 2009) and some field and geochronologic studies (Bloom et al., 1974; Esat et al., 1999; O'Leary et al., 2013; Schellmann and Radtke, 2004; Speed and Cheng, 2004; Stein et al., 1993; Thompson et al., 2011) indicate that there could have been at least two separate high stands of sea within the last interglacial period. In contrast, other modeling studies (Dutton and Lambeck, 2012; Lambeck et al., 2012) as well as field studies (Dutton et al., 2015; Muhs et al., 2002a, 2002b, 2011, 2012a, 2012b, 2014b; Stirling et al., 1998) do not indicate definitive evidence of more than a single high-sea stand during the last interglacial period.

Finally, there has been an increasing awareness of the importance of glacial isostatic adjustment (GIA) processes in understanding the Quaternary sea level record (e.g., Creveling et al., 2015; Lambeck et al., 2012; Milne and Mitrovica, 2008; Potter and Lambeck, 2003; Tamisiea and Mitrovica, 2011). These studies indicate that southern Cuba, due to its location relative to North American ice sheets, could have experienced a measureable, but modest departure from a purely eustatic sea level history during the late Quaternary, not as dramatic as a near-field locality such as Bermuda, but different from a far-field locality such as Barbados. Thus, if the late Quaternary uplift rate in the Guantanamo Bay area is low, as hypothesized, we should not expect to find reef terraces dating to the ~100 ka (MIS 5.3) or ~80 ka (MIS 5.1) sea stands.

2. Methods

Meinzer's (1933) map of the coral reef terraces around Guantanamo Bay was georeferenced successfully with modern satellite imagery and this was used as a mapping base. All delineations mapped as fossil coral reef deposits by Meinzer (1933) were checked in the field. Elevations of all localities studied were made using direct measurement by tape and hand level and/or by differential GPS measurements. GPS data were collected from at least four, and usually six to eight, satellites for at least 500 s to obtain consistent 3-D geometry. The data were post-processed using corrections against the closest active base stations. Differentially correcting the GPS elevations generally resulted in horizontal errors of 10 cm or less and vertical errors in the range of 20–80 cm. Our measurements use the CARIB97 high-resolution geoid height model for the Caribbean Sea region (Smith and Small, 1999). Comparison of GPS-derived elevation measurements with taped or hand-leveled elevation measurements shows good agreement, within the limits of instrumental uncertainty.

Sections exposing the Jaimanitas Formation were described and measured at a variety of localities around Guantanamo Bay (Fig. 3) and well-preserved corals were sampled for U-series dating. Corals used in this study were cleaned mechanically, washed in distilled water and X-rayed for aragonite purity. All samples are at least 95% aragonite and most are 98–100% aragonite (Table 1). After cleaning, sample preparation followed methods outlined by Ludwig et al. (1992) which are summarized briefly here. Cleaned corals were dissolved in HNO_3, spiked with ^{229}Th, ^{233}U, and ^{236}U and purified with ion-exchange methods. Purified U and Th were loaded with colloidal graphite on separate Re filaments and isotopic abundances were determined by thermal ionization mass spectrometry (TIMS). The U-Th spike is calibrated against a solution of uranium ore from the Schwartzwalder Mine that has yielded concordant U/Pb ages (Ludwig et al., 1985) and sample-to-sample agreement of ^{234}U/^{238}U and ^{230}Th/^{238}U (Ludwig and Paces, 2002). In addition, an in-house, carefully homogenized, aragonitic fossil coral of last interglacial age (~120 ka) was used for run-to-run checks. Ages were calculated using a half-life of 75,584 yr for ^{230}Th and a half-life of 245,620 yr for ^{234}U (Cheng et al., 2013).

3. Results

3.1. Coral reef distribution, stratigraphy, paleontology, and elevations

Meinzer (1933) reported two coral reef terraces in the Guantanamo Bay area. The oldest terrace is described as occurring at ~38 m above sea level and consists only of a small patch of limestone north of the modern runway on the leeward (western) side of the bay, covering an area of ~0.32 km by ~0.24 km, centered at about N19°54.6′ and W75°13′. The elevation of this terrace, measured by us, is ~39–40 m above sea level, and the reef consists of corals dominated by *Diploria* and *Orbicella* (the new genus *Orbicella* includes all species of the former *Montastraea*, with the exception of *M. cavernosa*; see Budd et al. (2012)). All corals we examined from this fossil reef are recrystallized and thus not collected for any analytical work.

A lower-elevation fossil reef rims much of Guantanamo Bay and was described by Meinzer (1933) as a terrace at ~12 m above sea level. Our field studies conducted around Guantanamo Bay show that Meinzer's (1933) mapping of this lower terrace is very accurate and we made very few modifications to his delineations. The formation is widely distributed around the bay (Fig. 3) and much of the U.S. Naval base is built directly on the upper part of the emergent coral reef.

The limestone that forms this low terrace, the Jaimanitas Formation, varies spatially in its sedimentology and paleontology. We recognize both an exposed, outer-coast facies (Figs. 4 and 5) and a protected, inner bay (lagoonal) facies (Fig. 6). On the outer, exposed part of the coast (Kittery Beach to Glass Beach and Leeward Point to Chapman Beach; Fig. 3), the deposits consist of corals, rare mollusks, and occasional bedrock clasts within a matrix of carbonate sand. The deposits are up to 12 m thick, and the outer parts host *Acropora palmata* corals in growth position (Fig. 5a,c). Landward of the *A. palmata* reefs, growth-position occurrences of *Orbicella nancyi*, *Montastraea cavernosa*, and *Siderastrea* are common and are beautifully exposed at a number of localities (Fig. 5b,d). *Orbicella nancyi* is one of two locally extinct Pleistocene coral species that lived in the Caribbean region during past interglacial periods (Pandolfi, 2007; Pandolfi et al., 2001). This taxon was previously referred to as “organ pipe” *Orbicella*, based on its appearance in the field. The other locally extinct species, *Pocillopora palmata*, superficially looks somewhat like *Orbicella nancyi* from a distance in the field (see Fig. 5.1 of Pandolfi et al., 2001) and colonies can be of approximately the same size as *O. nancyi*. However, close examination of the Guantanamo corals with an organ-pipe structure reveals corallites of ~2–2.5 mm diameter with ~24 septa, similar to *Orbicella annularis*. This indicates that the Cuban specimens are not *P. palmata*, which has smaller corallites (~1 mm) and lacks septa (Budd et al., 1994).

Outer-coast localities in a few places are constructional reefs built on what appears to be a wave-cut platform, such as that seen at Girl Scout Beach (Fig. 4b). At Chapman Beach, what we also interpret as a wave-cut platform on Tertiary conglomerate hosts an upward-growing sequence of *Acropora palmata* corals in the lower 4–5 m, capped by smaller, growth-position colonies of *Orbicella* in the upper ~2 m, at an elevation of 14.8 m (Fig. 7). Elsewhere, marine deposits at the inner edges of the outer-coast facies reef deposits are as high as 14.3 m above sea level on the eastern side of the bay (Figs. 4a and 5a).

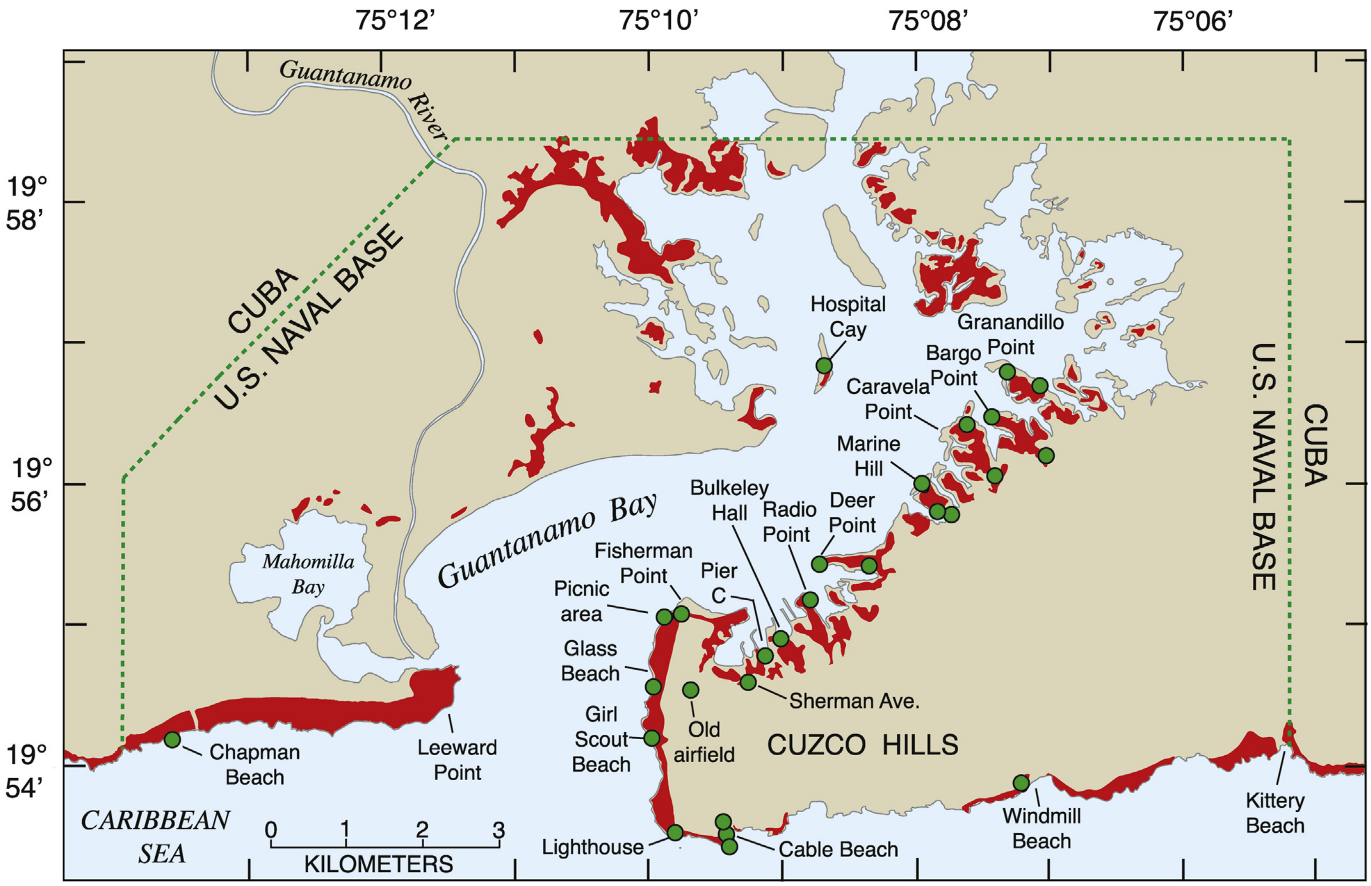

Fig. 3. Map showing the extent of the Jaimanitas Formation (emergent coral reef limestone) in the Guantanamo Bay area, slightly modified from Meinzer (1933) after field checking by the authors. Green circles are localities where GPS elevations were measured and corals collected. (For interpretation of the references to colour in this figure legend, the reader is referred to the web version of this article.)

In the more protected, lagoonal parts of Guantanamo Bay, between Fisherman Point and Granandillo Point (Fig. 3), the Jaimanitas Formation is composed of constructional coral reefs, typically 7–10 m thick (Fig. 6). These deposits lack *Acropora palmata*, but are characterized by growth-position *Orbicella nancyi* colonies up to 2 m high, as well as smaller, growth-position colonies of *Orbicella annularis*, *M. cavernosa*, *Siderastrea*, *Diploria*, and *Porites*. The upper 2–3 m of the formation in such protected areas also contain, at several localities, abundant thickets of *Acropora cervicornis*, but all of these we examined are no longer in growth position. These dense accumulations of dominantly *A. cervicornis* branches appear to have accumulated from simple collapse, similar to what has been described by Speed and Cheng (2004) on Barbados. If so, then it is unlikely that the corals have experienced significant horizontal transport or reworking. Mollusks are also abundant in the lagoonal facies of the Jaimanitas Formation and include paired bivalves and a number of gastropods, described in detail by Portell et al. (2008).

As discussed earlier, a number of studies have proposed that there were at least two separate high stands of sea during the last interglacial period. A complex last-interglacial sea-level history of this sort has been proposed for both tectonically stable coasts, such as the Bahamas and Australia (Thompson et al., 2011; O'Leary et al., 2013) and tectonically rising coasts, such as New Guinea and Barbados (Bloom et al., 1974; Esat et al., 1999; Schellmann and Radtke, 2004; Stein et al., 1993). With the possibility that the low (~12 m) terrace around Guantanamo Bay could date to the last interglacial period, we sought field evidence of a possible dual high-sea stand. Such evidence could be stratigraphic (two distinct reefs in vertical superposition, with a paleosol or karst-dominated surface between the two) or geomorphic (two or more distinct reef terraces, separated by a paleo-sea cliff). We found neither stratigraphic nor geomorphic evidence of more than one high-sea stand around Guantanamo Bay. In all sections we examined, we found no paleosols or contacts with karst features that could indicate subaerial exposure. At exposures of both protected, lagoonal reef facies and exposed, outer-coast reef facies, we found coral heads in growth position throughout all or most of the vertical extent of the sections exposed, indicating consistent upward reef growth during a single high-sea stand.

For exposed, outer-coast localities, the best estimate of relative paleo-sea level is defined by the elevation of the highest landward position of marine deposits lying above the wave-cut platform. At Windmill Beach, Cable Beach, the Lighthouse, and Fisherman Point, there is evidence of a wave-cut bench landward of the constructional reef, overlain by reworked and broken corals (Fig. 4b and c). If this interpretation is correct, then these innermost elevations mark maximum shoreline positions of erosional marine terraces. In California (cf. Muhs et al., 2012b, 2014b), the junction of the wave-cut platform and the backing sea cliff is called the shoreline angle and provides a close approximation of paleo-sea level. In the Guantanamo Bay area, our elevation measurements of the inner edges of outer-coast terrace deposits are likely maximum estimates of paleo-sea level, because the actual shoreline angles are not exposed. Elevations of the most landward marine deposits at these inner edges are as high as 14.3 m (Figs. 4a and 5a). In contrast, the protected, lagoonal facies deposits exposed between Pier C and

Table 1
Study localities, genera, aragonite contents, U and ^{232}Th concentrations, isotope activity ratios, and uranium-series ages of corals from Guantanamo Bay, Cuba. Samples in bold are those corals that best meet the criteria (U concentrations within range of modern corals, low ^{232}Th concentrations, and initial $^{234}U/^{238}U$ values close to the range for modern seawater) for closed-system histories and have the most reliable ages.

Sample	Genus or species	Aragonite (%)	Growth position?	Depth (m)[a]	U ppm	±	^{232}Th ppm	$^{230}Th/^{232}Th$	$^{234}U/^{238}U$ AR[b]	±	$^{230}Th/^{238}U$ AR	±	$^{230}Th/^{238}U$ Age (ka)[c]	±	$^{234}U/^{238}U$ initial AR[d]	±
WINDMILL BEACH, modern corals from supratidal beach deposits: N19.89892°, W75.11832°																
Cuba 16-1	*Orbicella annularis*	100	No	NA	2.30	0.11	0.0010	195	1.1507	0.0015	0.0285	0.0006	2.73	0.06	1.1519	0.0015
Cuba 16-2	*Orbicella annularis*	100	No	NA	2.32	0.11	0.0006	140	1.1451	0.0021	0.0116	0.0015	1.11	0.15	1.1456	0.0021
Cuba 16-3	*Orbicella annularis*	100	No	NA	2.75	0.11	0.0001	274	1.1515	0.0015	0.0038	0.0007	0.36	0.06	1.1516	0.0015
Cuba 16-4	*Orbicella annularis*	100	No	NA	2.62	0.11	0.0002	339	1.1504	0.0017	0.0106	0.0010	1.01	0.09	1.1508	0.0017
Cuba 16-5	*Orbicella annularis*	99	No	NA	3.02	0.11	0.0023	3190	1.1217	0.0017	0.8007	0.0026	131.7	0.90	1.1765	0.0023
Cuba 16-6	*Montastraea cavernosa*	100	No	NA	2.50	0.11	0.0026	28	1.1475	0.0017	0.0093	0.0010	0.88	0.10	1.1479	0.0017
CABLE BEACH, modern corals from supratidal beach deposits: N19.89269°, W75.15642°																
Cuba 30-A	*Siderastrea* sp.	100	No	NA	2.62	0.11	0.0000	0	1.1478	0.0016	x	x	x	x	1.1477	0.0016
Cuba 30-B	*Siderastrea* sp.	100	No	NA	2.35	0.12	0.0002	718	1.1434	0.0019	0.0224	0.0006	2.16	0.06	1.1438	0.0018
PIER C, west-facing ditch exposure: N19.91262°, W75.152455°; elevation of top = 11.4 m																
Cuba 9-1B	*Siderastrea* sp.	100	Yes	1.1	2.95	0.11	0.0001	87142	1.1108	0.0011	0.7702	0.0024	**125.1**	**0.7**	**1.1577**	**0.0015**
Cuba 9-1C	*Siderastrea* sp.	100	Yes	1.3	3.03	0.12	0.0002	46561	1.1158	0.0017	0.7811	0.0018	127.1	0.7	1.1658	0.0022
Cuba 9-1D	*Siderastrea* sp.	99	Yes	1.6	3.09	0.12	0.0001	48811	1.1190	0.0015	0.7805	0.0029	126.2	0.9	1.1699	0.0020
Cuba 9-1E	*Siderastrea* sp.	100	Yes	1.7	3.02	0.11	0.0002	36197	1.1169	0.0013	0.7829	0.0018	127.4	0.6	1.1675	0.0018
Cuba 9-1F	*Siderastrea* sp.	99-100	Yes	1.9	2.87	0.12	0.0002	31808	1.1112	0.0012	0.7638	0.0024	**123.1**	**0.8**	**1.1574**	**0.0016**
Cuba 9-1H	*Siderastrea* sp.	99	Yes	2.7	2.99	0.11	0.0006	12603	1.1215	0.0015	0.7879	0.0024	127.8	0.8	1.1743	0.0019
PIER C, east-facing road cut exposure: N19.91275°, W75.15227°; elevation of top = 9.9 m																
Cuba 9-4a	*Siderastrea* sp.	98	Yes	2.6	2.86	0.12	0.0021	3248	1.1141	0.0017	0.7844	0.0027	128.5	0.9	1.1641	0.0022
Cuba 9-4a rpt	*Siderastrea* sp.	98	Yes	2.6	2.83	0.11	0.0012	5469	1.1163	0.0016	0.7868	0.0017	128.8	0.6	1.1672	0.0021
Cuba 9-4	*Siderastrea* sp.	99	Yes	2.6	3.03	0.11	0.0002	36057	1.1169	0.0017	0.7820	0.0021	127.2	0.7	1.1674	0.0022
Cuba 9-5	*Siderastrea* sp.	99-100	Yes	3.2	2.99	0.11	0.0006	11267	1.1114	0.0019	0.7638	0.0022	123.1	0.8	1.1576	0.0025
Cuba 9-6	*Siderastrea* sp.	100	Yes	3.7	2.76	0.11	0.0001	82669	1.1104	0.0014	0.7809	0.0023	**128.4**	**0.8**	**1.1586**	**0.0019**
Cuba 9-7	*Siderastrea* sp.	100	Yes	4	2.69	0.11	0.0002	32097	1.1088	0.0018	0.7911	0.0026	**132.0**	**0.9**	**1.1579**	**0.0024**
Cuba 9-8	*Orbicella nancyi*	99	Yes	4.3	2.97	0.12	0.0029	2362	1.1138	0.0014	0.7563	0.0018	120.4	0.6	1.1598	0.0019
Cuba 9-9	*Orbicella nancyi*	98-99	Yes	4.7	2.39	0.11	0.0003	24224	1.1259	0.0015	0.8363	0.0028	142.0	1.0	1.1880	0.0020
Cuba 9-11	*Orbicella annularis*	100	Yes	5.7	2.24	0.11	0.0010	5893	1.1193	0.0013	0.8293	0.0033	141.6	1.2	1.1779	0.0019
Cuba 9-12	*Orbicella annularis*	99	No	5.8	2.49	0.11	0.0001	56755	1.1161	0.0015	0.8059	0.0026	134.8	0.9	1.1698	0.0020
Cuba 9-13	*Montastraea cavernosa*	99-100	Yes	6.2	2.71	0.11	0.0001	117481	1.1124	0.0014	0.8130	0.0020	138.1	0.8	1.1660	0.0020
Cuba 9-14	*Siderastrea* sp.	98-99	Yes	6.4	2.72	0.13	0.0095	672	1.1073	0.0017	0.7746	0.0024	127.2	0.8	1.1537	0.0022
Cuba 9-15	*Eusmilia fastigata*	99	No?	6.6	2.16	0.11	0.0013	3954	1.1120	0.0014	0.7735	0.0026	125.8	0.9	1.1598	0.0019
Cuba 9-16	*Siderastrea* sp.	100	Yes	6.8	2.57	0.11	0.0005	11694	1.1137	0.0014	0.7793	0.0019	127.1	0.7	1.1628	0.0019
Cuba 9-17	*Porites* sp.	99	Yes	7.2	2.74	0.11	0.0038	1732	1.1065	0.0020	0.7920	0.0021	132.9	0.9	1.1549	0.0027
PIER C, early (1998) exploratory samples																
Cuba 1	*Siderastrea sideria*	100	?	0–7	2.61	0.12	0.0001	67332	1.1214	0.0018	0.7881	0.0026	127.9	0.9	1.1742	0.0024
Cuba 2	*Siderastrea sideria*	100	?	0–7	2.68	0.13	0.0004	15357	1.1243	0.0018	0.7878	0.0031	127.1	1.0	1.1780	0.0024
Cuba 3	*Solenastrea bournoni*	100	?	0–7	2.79	0.11	0.0000	197874	1.1153	0.0014	0.7751	0.0026	125.5	0.8	1.1643	0.0019
HOSPITAL CAY: N19.94774°, W75.14455°; elevation at top = 10.8 m																
Cuba 29-1	*Colpophyllia* sp.	100	Yes	~4.5	2.58	0.11	0.0001	63397	1.1086	0.0016	0.7487	0.0018	**119.4**	**0.6**	**1.1521**	**0.0020**
Cuba 29-2	*Orbicella nancyi*	98-99	Yes	~4.5	2.75	0.11	0.0025	2678	1.1195	0.0015	0.7952	0.0027	130.6	0.9	1.1727	0.0020
Cuba 29-3	*Siderastrea* sp.	99-100	Yes	~4.5	2.98	0.12	0.0003	21171	1.1084	0.0017	0.7795	0.0026	**128.5**	**0.9**	**1.1558**	**0.0022**
Cuba 29-4	*Colpophyllia* sp.	98-99	Yes	~4.5	2.56	0.11	0.0001	65619	1.1173	0.0017	0.7882	0.0019	128.9	0.7	1.1688	0.0022
ROADCUT NEAR OLD AIRFIELD: N19.90884°, W75.16146°; elevation of top = 9.4 m; seaward of this locality, elevation = 11.9 m																
Cuba 13-A	*Acropora cervicornis*	100	No		2.55	0.12	0.0003	17787	1.1086	0.0017	0.7819	0.0028	129.2	1.0	1.1563	0.0022
SOUTH OF SHERMAN AVENUE road cut exposure: N19.91034°, W75.15431°; elevation at top of inner edge = 14.0 m																

(*continued on next page*)

Table 1 (*continued*)

Sample	Genus or species	Aragonite (%)	Growth position?	Depth (m)[a]	U ppm	±	^{232}Th ppm	^{230}Th/^{232}Th	^{234}U/^{238}U AR[b]	±	^{230}Th/^{238}U AR	±	^{230}Th/^{238}U Age (ka)[c]	±	^{234}U/^{238}U initial AR[d]	±
Cuba 14-A	*Siderastrea* sp.	98–99	Yes	~1.5	3.65	0.12	0.0047	1898	1.1111	0.0014	0.8070	0.0023	136.5	0.9	1.1633	0.0020
Cuba 14-B	Siderastrea sp.	98–99	Yes	~1.5	3.33	0.12	0.0033	2361	1.1112	0.0018	0.7827	0.0024	128.8	0.8	1.1600	0.0024
CABLE BEACH cliff exposure: N19.89238°, W75.15642°; elevation at top of exposure = 11.6 m, inner edge at 14.3 m																
Cuba 23-7	*Diploria* cf. *D. strigosa*	96–97	Yes	3.6	2.63	0.11	0.0001	73058	1.1111	0.0017	0.7926	0.0020	131.9	0.8	1.1611	0.0022
Cuba 23-11	*Diploria* sp.	100	Yes	4.55	2.97	0.12	0.0001	71744	1.1152	0.0017	0.8017	0.0021	133.7	0.8	1.1679	0.0023
Cuba 23-6	*Diploria* sp.	100	Yes	4.9	2.88	0.13	0.0009	8171	1.1090	0.0021	0.7966	0.0027	133.7	1.0	1.1589	0.0028
Cuba 23-5	*Orbicella nancyi*	100	Yes	5.7	2.35	0.11	0.0001	68675	1.1301	0.0015	0.8676	0.0017	151.8	0.8	1.1996	0.0020
Cuba 23-5A	*Diploria* sp.	100	Yes	5.9	2.53	0.11	0.0003	23861	1.1017	0.0014	0.7858	0.0022	**132.2**	**0.8**	**1.1477**	**0.0019**
Cuba 23-4A	*Siderastrea* sp.	100	Yes	6.3	2.95	0.11	0.0000	171243	1.1218	0.0013	0.7994	0.0025	131.3	0.8	1.1764	0.0018
Cuba 23-3	*Orbicella nancyi*	99	Yes	7.35	2.32	0.11	0.0001	95381	1.1323	0.0016	0.8506	0.0026	145.1	1.0	1.1992	0.0022
Cuba 23-2	*Diploria* sp.	100	Yes	7.35	3.08	0.11	0.0004	16446	1.1072	0.0016	0.7909	0.0021	**132.3**	**0.8**	**1.1558**	**0.0021**
Cuba 23-1	*Diploria* sp.	100	Yes	7.8	2.48	0.11	0.0001	73156	1.1096	0.0017	0.7959	0.0021	**133.3**	**0.8**	**1.1597**	**0.0022**
CABLE BEACH, cliff exposure, ~30 m to the north of main exposure: N19.89252°, W75.15656°																
Cuba 23-10	*Diploria* cf. *D. strigosa*	100	Yes		2.86	0.11	0.0001	122490	1.1098	0.0014	0.7729	0.0028	**126.2**	**0.9**	**1.1567**	**0.0019**
MARINE HILL, outer part, staircase cut exposure: N19.93283°, W75.13214°; elevation of top = 9.56 m																
Cuba 7-2	*Porites* cf. *P. asteroides*	99	?	0.9	2.94	0.11	0.0018	3988	1.1170	0.0012	0.8014	0.0022	133.1	0.8	1.1704	0.0017
Cuba-7-3A	*Siderastrea* sp.	99	Yes	0.8	2.90	0.11	0.0002	33759	1.1175	0.0016	0.7914	0.0028	129.9	0.9	1.1696	0.0021
Cuba 7-3B	*Siderastrea* sp.	100	Yes	0.9	2.95	0.12	0.0002	32483	1.1195	0.0015	0.7760	0.0023	124.8	0.7	1.1700	0.0019
Cuba-7-3C	*Siderastrea* sp.	99	Yes	1	2.86	0.12	0.0004	14982	1.1204	0.0017	0.7741	0.0022	124.0	0.7	1.1709	0.0022
Cuba7-3D	*Orbicella* sp.	99	Yes	1.2	2.94	0.11	0.0001	106048	1.1387	0.0014	0.8403	0.0026	139.8	0.9	1.2057	0.0019
Cuba 7-4	*Siderastrea* sp.	100	Yes	5.2	3.69	0.13	0.0001	94913	1.1293	0.0014	0.6108	0.0019	83.3	0.4	1.1636	0.0016
Cuba 7-5	*Siderastrea* sp.	99	Yes	7	3.23	0.11	0.0003	22657	1.1067	0.0017	0.6478	0.0019	94.2	0.5	1.1392	0.0021
Cuba 7-6	*Siderastrea* sp.	99	Yes	7.2	3.27	0.12	0.0003	25150	1.1024	0.0034	0.6394	0.0019	92.9	0.7	1.1330	0.0043
Cuba-7-7	*Orbicella nancyi*	98–99	Yes	7.9	2.71	0.11	0.0003	21420	1.1165	0.0015	0.6752	0.0025	99.0	0.6	1.1540	0.0018
Cuba 7-8	*Diploria* sp.	99	?	8.2	2.34	0.11	0.0001	49248	1.1117	0.0014	0.7292	0.0019	113.4	0.6	1.1538	0.0019
MARINE HILL, inner part, road cut exposure: N19.92992°, W75.12940°; elevation of top = 10.8 m																
Cuba 8-1	*Orbicella annularis*	99–100	Yes	0.2	3.53	0.11	0.0001	66659	1.1260	0.0019	0.6736	0.0018	97.2	0.5	1.1658	0.0024
Cuba 8-2	*Siderastrea* sp.	99	?	0.7	3.36	0.11	0.0002	29773	1.1148	0.0018	0.6668	0.0014	97.3	0.4	1.1511	0.0022
Cuba 8-3-a	*Acropora cervicornis*	99	No	0.7	8.99	0.12	0.0012	11997	1.1091	0.0018	0.5210	0.0011	68.3	0.3	1.1323	0.0021
Cuba 8-3-a rpt	*Acropora cervicornis*	99	No	0.7	7.63	0.12	0.0008	16952	1.1262	0.0018	0.6210	0.0015	85.7	0.4	1.1607	0.0022
Cuba 8-4	*Siderastrea* sp.	95	Yes	1.6	3.19	0.11	0.0010	7405	1.1122	0.0017	0.7620	0.0017	122.4	0.6	1.1584	0.0022
CHAPMAN BEACH cliff exposure: N19.90351°, W75.22624°; elevation at top = 14.8 m																
Cuba-31-10	*Orbicella* sp.	98	Yes	0.7	2.93	0.11	0.0001	95742	1.1356	0.0015	0.8741	0.0048	152.3	1.8	1.2085	0.0022
Cuba-31-11	*Orbicella* sp.	98–99	Yes	1.6	3.34	0.11	0.0002	48644	1.1723	0.0016	0.9792	0.0031	180.7	1.5	1.2870	0.0024
Cuba 31-8	*Acropora palmata*	99	Yes	5.1	4.56	0.11	0.0006	15204	1.1263	0.0017	0.6910	0.0020	101.2	0.5	1.1680	0.0021
Cuba-31-6	*Acropora palmata*	98–99	Yes	5.5	3.77	0.11	0.0001	164592	1.1203	0.0015	0.7596	0.0020	119.9	0.6	1.1688	0.0019
Cuba-31-5	*Acropora palmata*	99	Yes	5.7	3.66	0.12	0.0038	2465	1.1380	0.0015	0.8453	0.0030	141.6	1.1	1.2058	0.0020
Cuba 31-4	*Acropora palmata*	100	Yes	5.9	3.70	0.11	0.0001	61934	1.1008	0.0017	0.7019	0.0020	108.3	0.6	1.1368	0.0021
Cuba 31-3	*Acropora palmata*	100	Yes	6.4	4.31	0.11	0.0002	35988	1.1084	0.0016	0.6588	0.0017	96.5	0.5	1.1423	0.0019
Cuba-31-2	*Acropora palmata*	99	Yes	6.8	3.93	0.11	0.0001	137563	1.1096	0.0013	0.7049	0.0015	107.4	0.5	1.1484	0.0017
Cuba 31-1	*Acropora palmata*	99	Yes	7.2	3.94	0.11	0.0001	76982	1.1099	0.0014	0.7698	0.0029	**125.2**	**0.9**	**1.1564**	**0.0019**

[a] Depth from top of the exposure.
[b] AR = activity ratio; errors are two-sigma.
[c] Calculated using half-lives of 75,584 yr for ^{230}Th and 245,620 yr for ^{234}U (Cheng et al., 2013); errors are two-sigma.
[d] Back-calculated initial ^{234}U/^{238}U value using ^{230}Th/238U age and measured ^{234}U/^{238}U value; errors are two-sigma.

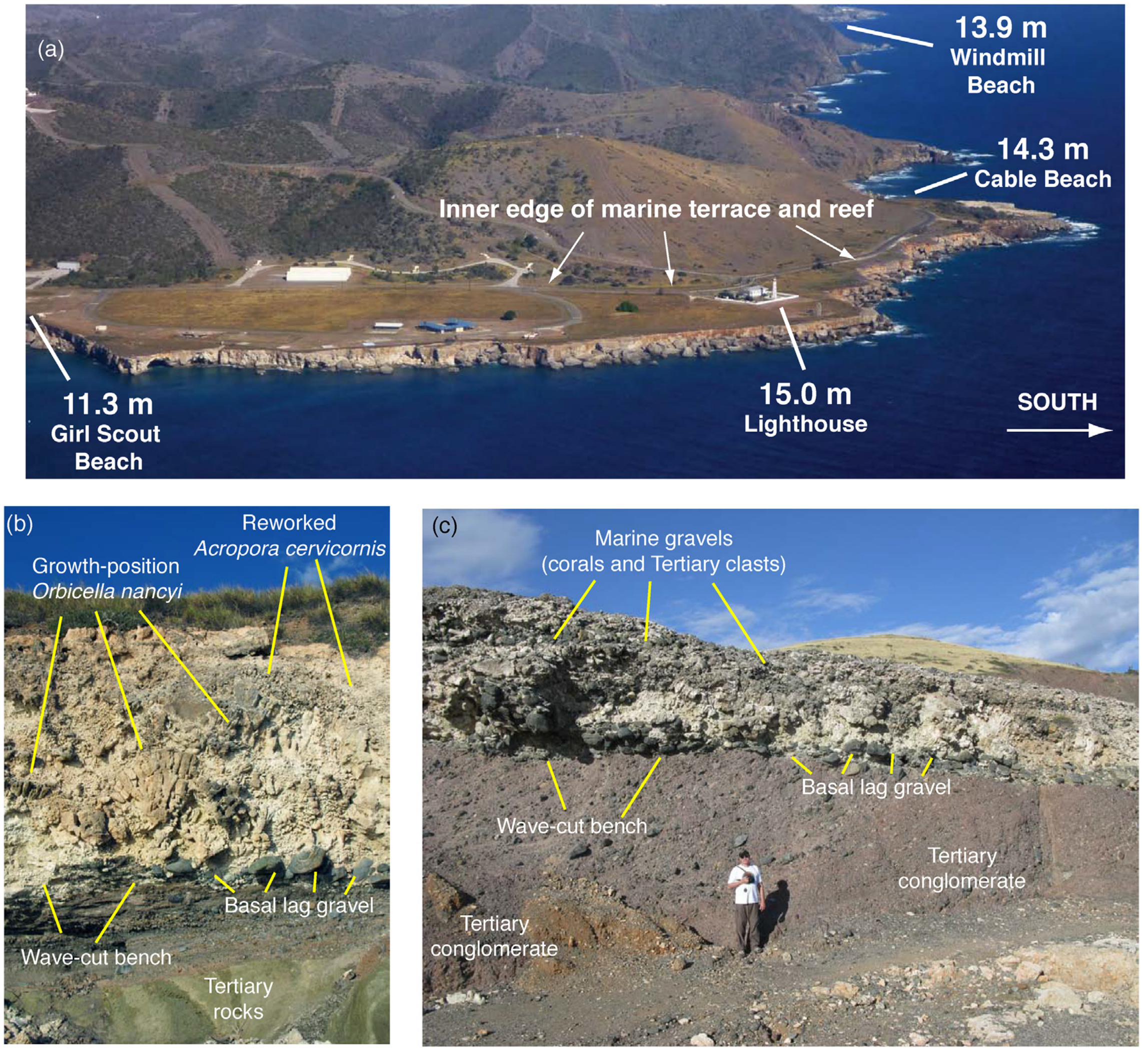

Fig. 4. (a) Oblique aerial photograph of the eastern, windward part of Guantanamo Bay, from Girl Scout Beach to Windmill Beach (see Fig. 3), showing the reef terrace geomorphology. (b) Cliff exposure at Girl Scout Beach (see Fig. 3 for location), showing, from bottom to top, Tertiary sedimentary rocks, wave-cut bench, basal marine lag gravels, growth-position corals (*Orbicella nancyi*), and reworked corals. (c) Cliff exposure on the eastern side of Cable Beach (see Fig. 3 for location), showing, from bottom to top, Tertiary conglomerate, wave-cut bench, basal lag gravel, and marine gravels consisting of both coral fragments and clasts from Tertiary conglomerate; geologist in photo is 1.8 m tall.

Granandillo Point are composed almost entirely of growth-position corals and are therefore constructional landforms. Because corals must grow in some minimum depth of water, the highest elevations measured in the field are minimum estimates of paleo-sea level and require adjustment for coral habitat depth. Based on observations made by Shinn et al. (1989) in the nearby Florida Keys where the same coral taxa are found as in Cuba, *minimum* water depths for optimal growth of modern *Orbicella annularis*, *M. cavernosa*, *Diploria*, and *Siderastrea siderea* are ~3 m. Because *Orbicella nancyi* is extinct, there is no way to determine what correction might be appropriate for habitat depth for this species. In this study, we take a conservative approach and use the minimum water depth for optimal growth for the other genera (~3 m), as observed by Shinn et al. (1989). Following Muhs et al. (2011), we therefore add 3 m to our highest lagoonal facies elevations. Overall, results show that except for Chapman Beach, elevations of inner edges of outer-coast localities and habitat-depth-corrected elevations of protected, lagoonal localities are in good agreement, with apparent paleo-sea level elevations showing a narrow range between ~13 m and ~15 m (Fig. 8). Although the Chapman Beach locality is an outer, exposed reef locality (Fig. 3), there is no backing sea cliff that could define a shoreline angle. Nevertheless, the top of the reef complex at Chapman Beach is at 14.8 m above sea level and growth-position corals (*Orbicella* and *Diploria*) are found all the way to the top of the terrace. Thus, again assuming conservatively that these corals grew in water depths of at least ~3 m, this gives a corrected, apparent paleo-sea level elevation of ~17.8 m.

3.2. Uranium-series dating

We collected modern specimens of corals from supratidal beach drift at Windmill Beach and Cable Beach and fossil corals for uranium-series dating at Cable Beach, Chapman Beach, Hospital Cay, Marine Hill, Pier C, and two localities near the old airfield, south of Pier C (Fig. 3). At Cable Beach, Chapman Beach, Marine Hill, and Pier C, corals were collected from the bottom to the top of each exposure, in part to test our field interpretation that the entire deposit represents a single high-sea stand. In assessing the integrity of U-series ages, we consider the following criteria, established during the early years of U-series geochronology by Broecker and Thurber (1965) and still valid today: (1) absence of recrystallization of primary aragonite to calcite, based on both examination of

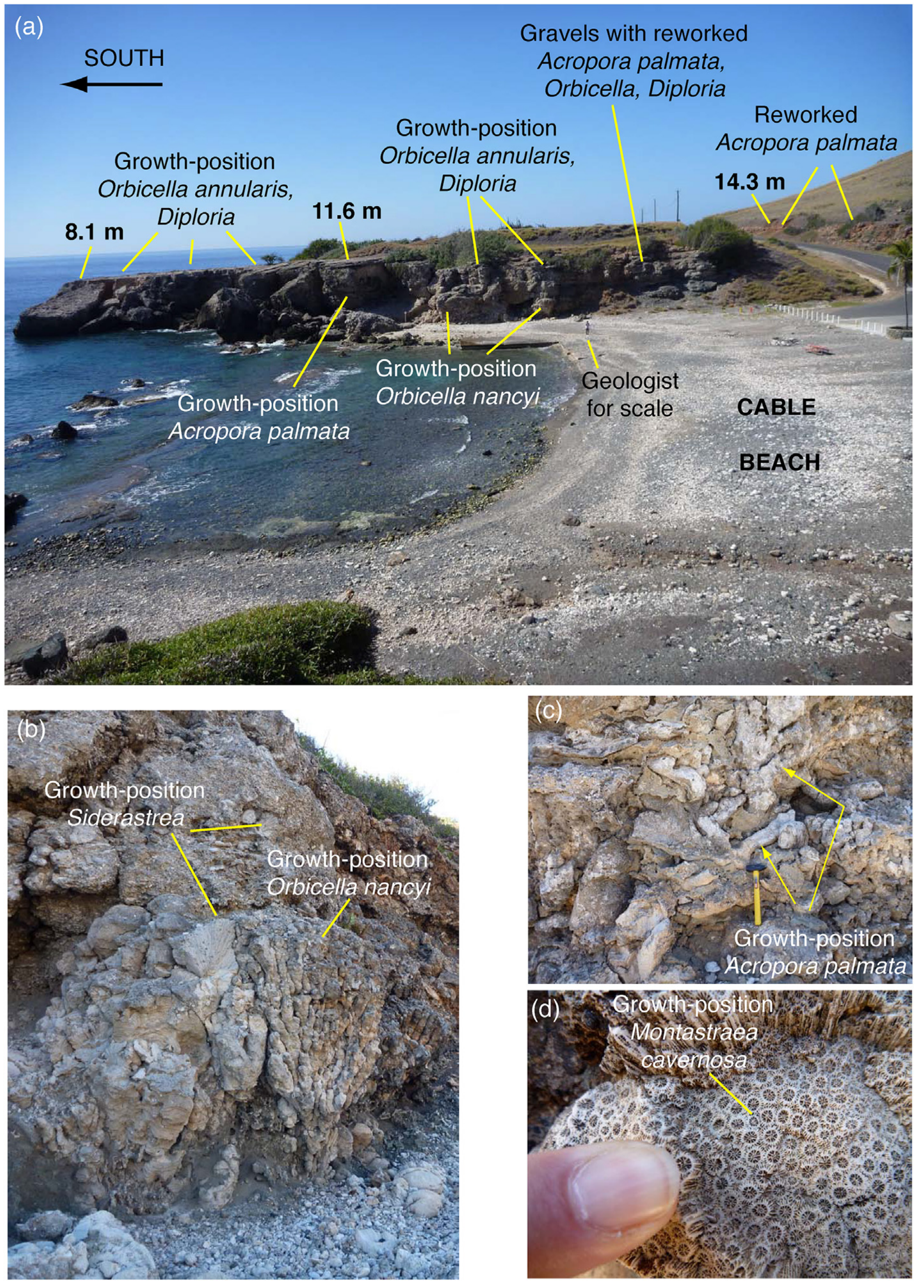

Fig. 5. (a) Photograph (looking west) of geomorphology and cliff exposure of the exposed, outer-coast facies of the Jaimanitas Formation at Cable Beach (see Fig. 3), with measured elevations and dominant coral taxa. (b) Close-up of growth-position *Orbicella nancyi* colony and other corals found in lower part of cliff exposure shown in (a). (c) Close-up view of growth-position *Acropora palmata* corals shown in lower part of cliff exposure shown in (a). (d) Close-up view of growth-position *Montastraea cavernosa* coral shown in lower part of cliff exposure shown in (a).

samples under magnification and X-ray diffraction analyses; (2) verification that ^{230}Th measured is due to in situ radioactive decay of parent ^{234}U and not from detrital silicate contaminants, confirmed by low concentrations of ^{232}Th and high values of ^{230}Th/^{232}Th; (3) verification that bulk U concentrations are within the range of modern samples of the same species, indicating that there has been no gain or loss of U since deposition; and (4) measured ^{234}U/^{238}U values that, when combined with apparent ^{230}Th/^{234}U ages, yield back-calculated initial ^{234}U/^{238}U values that fall within the range of modern seawater. Regarding criterion (1), one sample (Cuba 8-4) is 95% aragonite and one other (Cuba 23-7) is 96–97% aragonite; all others are 98–100% aragonite and most are 99–100% aragonite (Table 1). Apart from the modern beach-collected corals, criterion (2) is met for some but not all fossil corals. High ^{232}Th concentrations (and therefore low ^{230}Th/^{232}Th values) indicate significant inherited ^{230}Th from detrital silicate minerals and will bias samples to older apparent ages. The choice of what ^{232}Th concentration or which ^{230}Th/^{232}Th value to use as a threshold for determining whether there is significant contamination is typically chosen by the individual geochronologist. Thompson et al. (2011) considered corals with ^{232}Th concentrations of greater than 0.0004 ppm to have significant amounts of inherited ^{230}Th. The fossil corals in the present study have ^{232}Th concentrations ranging from 0 to 0.0095 ppm and ^{230}Th/^{232}Th values ranging from ~670 to ~171,000 (Table 1). Most corals with ^{232}Th concentrations of 0.0004 ppm or less have ^{230}Th/^{232}Th

Fig. 6. (a) Photograph (looking west) of the protected, lagoonal facies of the Jaimanitas Formation exposed at Pier C (see Fig. 3) and dominant coral taxa. (b), (c), (d) Close-up photographs of common coral taxa found in the exposure shown in (a) between depths of 3–4 m. Knife in photos is 5.5 cm long.

values > 14,000 (Cuba 8-3-a [rpt] and 31-8 also have ^{230}Th/^{232}Th values > 14,000, but have ^{232}Th values slightly >0.0004). The high ^{230}Th/^{232}Th values and low concentrations of ^{232}Th indicate that many, but not all of the corals contain little or no contaminating silicate mineral material, but we address this issue in more detail below. With some exceptions (e.g., Thompson et al., 2011), U-series geochronologists often overlook criterion (3), bulk U content, in their interpretations and regrettably some investigators do not even report such data. However, secondary additions of bulk U will bias samples to younger apparent ages and U loss will bias samples to older apparent ages. Modern and Holocene specimens of *Orbicella*, *Siderastrea*, *Diploria*, and *Porites* have U concentrations of 2–3 ppm (Table 1; see also Cross and Cross, 1983; Chen et al., 1991; Ludwig et al., 1996; Muhs et al., 2011). Fossil specimens of *Siderastrea* with apparent closed-system histories sometimes have U contents slightly higher than 3 ppm (Martin et al., 1988; Gallup et al., 2002; Muhs et al., 2002a, 2014a; Speed and Cheng, 2004). In contrast, modern and Holocene species of *Acropora* (*A. palmata* and *A. cervicornis*) have U concentrations of 3.0–3.8 ppm (Bard et al., 1990; Chen et al., 1991; Cross and Cross, 1983; Gallup et al., 1994; Hamelin et al., 1991; Thompson et al., 2011).

Finally, the best criterion for determining closed-system conditions during the post-emergence history of a fossil coral is concordance between ^{230}Th/^{234}U and ^{231}Pa/^{235}U ages (Edwards et al., 1997, 2003). We did not determine ^{231}Pa/^{235}U ages for our samples, nor do most U-series laboratories. However, another measure for closed-system history, criterion (4) given above, is a determination of whether the back-calculated initial ^{234}U/^{238}U value of a sample, based on its present measured ^{234}U/^{238}U value and the ^{230}Th/^{234}U age, is within the range of modern seawater. Modern seawater, commonly cited as having an "average" ^{234}U/^{238}U value of 1.149, actually has a significant range of values, from 1.140 to 1.155 (Chen et al., 1986; Delanghe et al., 2002). Indeed, modern corals we collected on two beaches in the Guantanamo Bay area have ^{234}U/^{238}U values ranging from 1.143 to 1.152 (Table 1). Evaluation of back-calculated initial ^{234}U/^{238}U values has become, within the U-series geochronology community, the most commonly used measure for assessing closed-system history in U-series geochronology. Nevertheless, it is important to point out that this parameter has limitations. For example, Edwards et al. (1997) report that some corals with initial ^{234}U/^{238}U activity values as high as 1.166 show concordance between ^{230}Th/^{234}U and ^{231}Pa/^{235}U ages. Conversely, Gallup et al. (2002) and Cutler et al. (2003) report a number of corals they analyzed that have "acceptable" back-calculated initial ^{234}U/^{238}U values, but do *not* show concordance between ^{230}Th/^{234}U and ^{231}Pa/^{235}U ages. Gallup et al. (1994) point out that samples with elevated initial ^{234}U/^{238}U values from within the same reef terrace tend to yield older apparent ages and other studies have borne out this interpretation. On a ^{230}Th/^{238}U vs. ^{234}U/^{238}U evolution diagram, such samples will plot above a theoretical isotope evolution pathway. Corals from both the present study (Fig. 9a) and those from the nearby Florida Keys (Fig. 9b), reported by Muhs et al. (2011), display the same tendency described by Gallup et al. (1994) in their study of Barbados corals. In the present study, we consider uncorrected ages calculated for fossil corals to be at least *approximately* accurate if they pass criteria

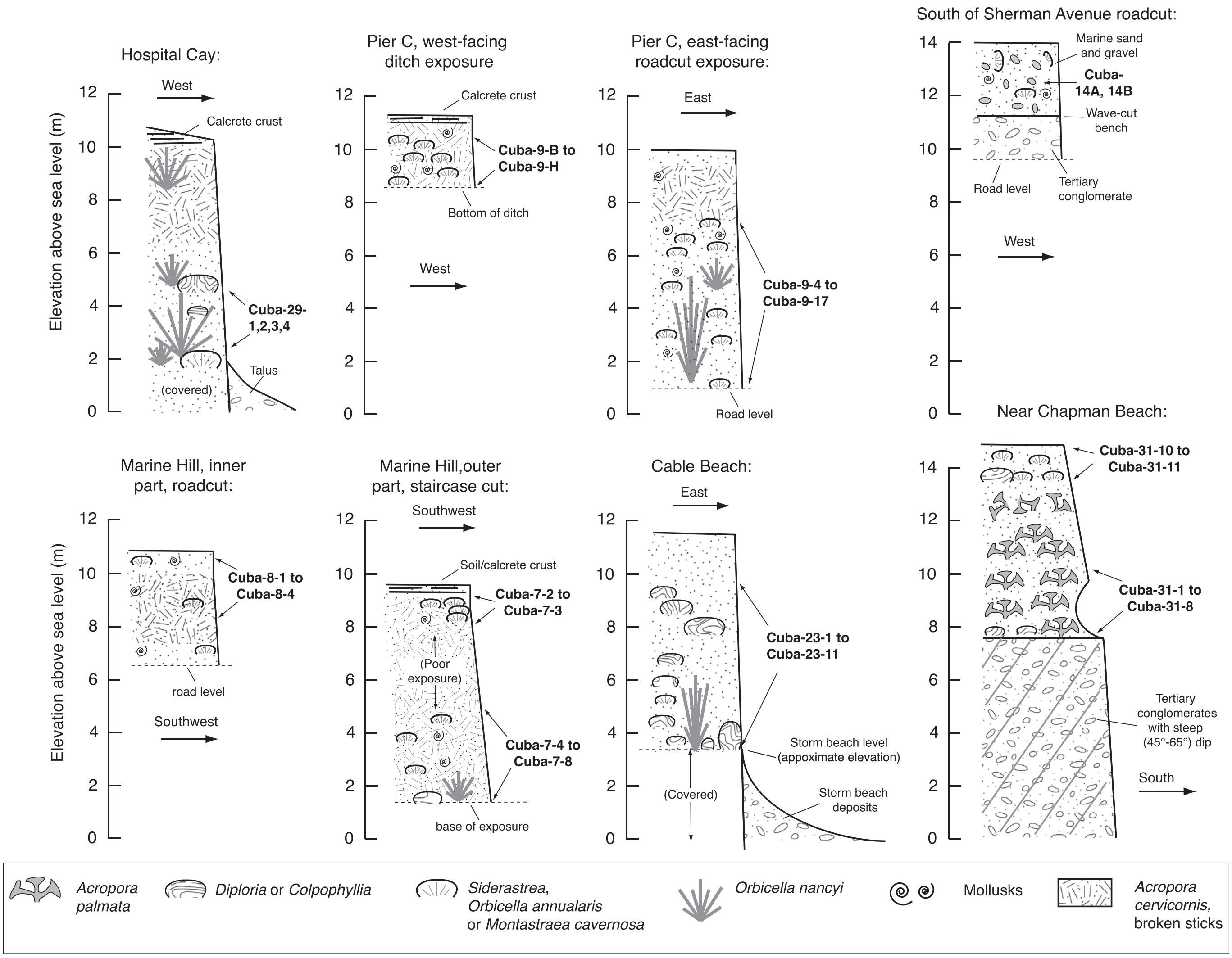

Fig. 7. Cliff sections and roadcut exposures of the Jaimanitas Formation in the Guantanamo Bay area (locations shown in Fig. 3), scaled to sea level, showing sedimentology, dominant coral taxa, and sample numbers (keyed to Table 1).

(1), (2), and (3), described above, and in addition have back-calculated initial $^{234}U/^{238}U$ activity values from 1.147 to 1.159 (following Stirling et al., 1998). This range of $^{234}U/^{238}U$ activity values is only slightly higher than the reported range of values in modern seawater but is consistent with the range in these values that Edwards et al. (1997) report for corals with concordant $^{230}Th/^{234}U$ and $^{231}Pa/^{235}U$ ages.

Modern (dead) corals collected from supratidal deposits at Windmill Beach and Cable Beach (Fig. 3) have U concentrations similar to those reported elsewhere and measured $^{234}U/^{238}U$ values that fall into the range of modern seawater (Table 1). *Orbicella annularis* and *Montastraea cavernosa* from Windmill Beach, with one exception, have U concentrations between 2.0 and 2.9 ppm, similar to what has been reported for living or modern-dead specimens of this genus elsewhere in the Caribbean and western Atlantic Ocean (Cross and Cross, 1983; Chen et al., 1991; Muhs et al., 2011). The one exception (Cuba 16-5) is an apparently reworked fossil derived from the nearby emergent marine deposits on the adjacent cliff, which gave an age of 131.7 ± 0.9 ka. At Cable Beach, two modern *Siderastrea* fragments gave U concentrations of 2.3–2.6 ppm, similar to what has been reported for modern specimens of this genus from Barbados and Bermuda (Cross and Cross, 1983; Ludwig et al., 1996). Overall, measured $^{234}U/^{238}U$ values in the modern corals range from 1.143 to 1.152, within the range of what has been reported for modern seawater (Delanghe et al., 2002).

For fossil corals at Guantanamo Bay, the best results, considering all the criteria described above, come from the protected, lagoonal facies exposures at Pier C (Figs. 3, 6 and 7). All samples collected from this section yielded U contents within the range of modern corals. Some samples have concentrations of ^{232}Th greater than 0.0004 ppm, indicating some amount of inherited ^{230}Th, using the criterion of Thompson et al. (2011). These include Cuba 9-1H, 9-4a, 9-5, 9-8, 9-11, 9-14, 9-15, 9-16, and 9-17. The oldest part of the section is the east-facing roadcut exposure and the lowest coral exposed (Cuba 9-17, at a depth of 7.2 m from the top of the exposure), a *Porites*, has an age of 132.9 ± 0.9 ka, with an initial $^{234}U/^{238}U$ value of 1.1549, indicating minimal bias to an older possible age. Continuing up-section, corals above this depth with initial $^{234}U/^{238}U$ values less than 1.159 range in age from 127.2 ± 0.8 ka (Cuba 9-14, at 6.4 m), 132.0 ± 0.9 ka (Cuba 9-7, at 4.0 m), 128.4 ± 0.8 ka (Cuba 9-6, at 3.7 m), and 123.1 ± 0.8 ka (Cuba 9-5, at 3.2 m). On the ditch exposure facing west, all samples except Cuba 9-1H are statigraphically above all the sampled corals on the east-facing

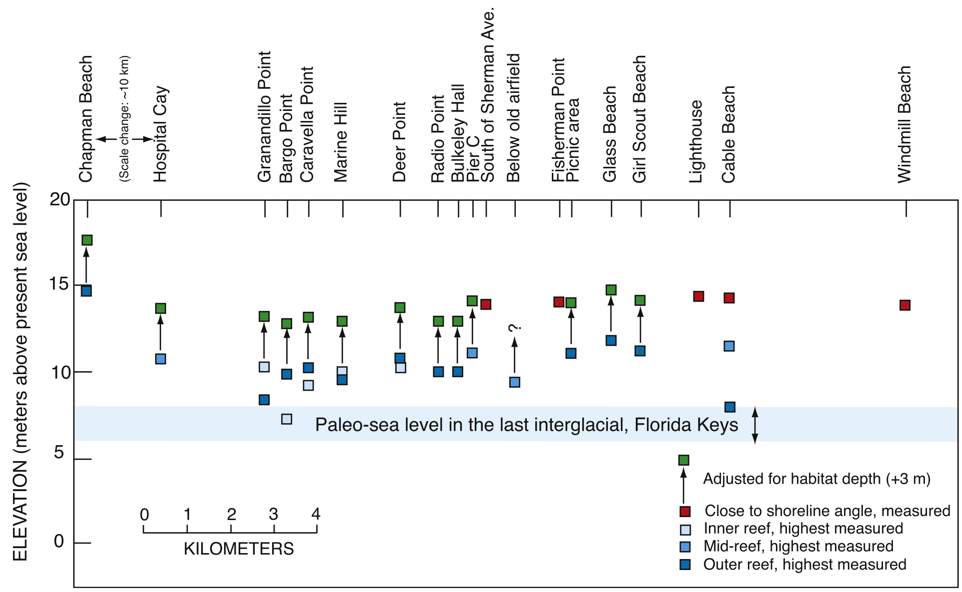

Fig. 8. Shore-parallel profile showing elevations of the Jaimanitas Formation reef limestone measured in this study (locations shown in Fig. 3). Note scale change between Chapman Beach and Hospital Cay; distance between these two localities is ~10 km. Blue shaded area shows estimated paleo-sea level during the last interglacial period, derived from the tectonically stable Florida Keys and Miami, Florida area (from Muhs et al., 2011). (For interpretation of the references to colour in this figure legend, the reader is referred to the web version of this article.)

exposure. The upper part of the west-facing ditch exposure has a *Siderastrea* at 1.9 m depth (Cuba 9-1F) with an age of 123.1 ± 0.8 ka and another *Siderastrea* at 1.1 m depth (Cuba 9-1B) with an age of 125.1 ± 0.7 ka, both with initial $^{234}U/^{238}U$ values less than 1.159. Corals at intermediate depths have similar apparent ages, but have slightly higher initial $^{234}U/^{238}U$ values. Taken at face value, all the corals in both exposures of Pier C fall into the range of ages for MIS 5.5 found on other coastlines, but do not have a clear stratigraphic integrity. Similar results were obtained from the corals collected between ~5 m and ~7 m depth from the protected, lagoonal facies exposure on Hospital Cay. Of the four corals sampled here, two (Cuba 29-3, 29-1) had initial $^{234}U/^{238}U$ values less than 1.159 and gave ages of 128.5 ± 0.9 ka and 119.4 ± 0.6 ka, respectively. The other two corals have elevated initial $^{234}U/^{238}U$ values and are likely biased old by some amount, but still fall into the age range of MIS 5.5.

Of the exposed, outer-coast facies localities, the best results come from Cable Beach (Figs. 3–5). With one exception (Cuba 23-2, with a slightly higher U content), all corals collected from this section yielded U contents within the range of modern corals and have very high $^{230}Th/^{232}Th$ values, indicating no significant amounts of inherited ^{230}Th. From this outcrop, three corals (Cuba 23-2, 23-5A, and 23-6) all have initial $^{234}U/^{238}U$ values less than 1.159 (Table 1; note, however, that Cuba 23-6 has a lower than optimal $^{230}Th/^{232}Th$). These corals have ages of 132.3 ± 0.8 ka (near the base of the exposure) and 132.2 ± 0.8 ka and 133.7 ± 1.0 ka 2–3 m above the base of the exposure. About 30 m inland (north) of the main exposure shown in Figs. 5b and 7, a growth-position *Diploria* (Cuba 23-10) was collected above a complex series of gravel layers and gave an age of 126.2 ± 0.9 ka with an initial $^{234}U/^{238}U$ value of 1.1567, indicating minimal age bias. The remaining corals from Cable Beach have slightly elevated initial $^{234}U/^{238}U$ values (Cuba 23-1, 4A, 7, 11) or more significantly elevated initial $^{234}U/^{238}U$ values (Cuba 23-3 and Cuba 23-5). With the exception of the latter two samples, all the corals from Cable Beach, as with those at Pier C and Hospital Cay, have ages that fall into the general age range of MIS 5.5.

In a roadcut exposure south of Sherman Avenue (Fig. 3), a bench is cut on Tertiary conglomerates and is overlain by ~2.6 m of marine deposits. The bench has an elevation of 11.4 m and the top of the marine deposits has an elevation, at its most-landward exposure, of 14.0 m. Within the marine deposits, clasts are composed of Tertiary rocks, transported coral fragments, and gastropods, including paired bivalves. However, we also found small coral heads, dominated by *Siderastrea*, apparently in growth position, on gravel clasts derived from Tertiary rocks. Two of these corals, Cuba 14-A and 14-B, have slightly elevated U contents (3.3–3.6 ppm) and initial $^{234}U/^{238}U$ values (1.1633 and 1.1600), but gave apparent ages of 136.5 ± 0.9 and 128.8 ± 0.8 ka, respectively. Less than a kilometer to the west, a roadcut exposure just east of the old airfield (Cuba 13-A) has a stratigraphy similar to that of Cuba-14, where a bench is cut on Tertiary conglomerates and is overlain by corals and mollusks, most of which are not in growth position. The top of the marine gravels has an elevation of 9.4 m. An *Acropora cervicornis* coral was collected from these gravels, but gave a U content of only 2.55 ppm, indicating probable U loss.

Less success was achieved with attempts to date corals at the other sections that were visited, Marine Hill (inner part), Marine Hill (outer part), and Chapman Beach (Figs. 3 and 7). Both of the Marine Hill sections are protected, lagoonal facies exposures. In the outer of these two outcrops, the top of the reef is at an elevation of 9.6 m, and ~8 m of reef carbonate can be seen. The reef here consists mostly of broken *Acropora cervicornis* sticks, with growth-position *Siderastrea* and less-common *Porites*, *Orbicella*, and *Diploria*. The interval from ~1.2 m down to ~5 m is poorly exposed and no samples were taken in this zone. In the upper 1.2 m, five corals (Cuba 7-2, 3A, 3B, 3C, and 3D) gave apparent ages of ~140 ka to ~124 ka, although all have high initial $^{234}U/^{238}U$ values and are likely biased old to one degree or another (Table 1). Nevertheless, these corals have high $^{230}Th/^{232}Th$ values and U contents that fall within the range (2–3 ppm) for modern specimens of these genera. At a depth of 5.2 m and below, all five corals sampled have significantly younger ages (~113 ka to ~83 ka), clearly at variance with the stratigraphy, even though all corals but one are in growth position. Three of these (Cuba 7-4, 5, 6) are *Siderastrea* specimens that have U contents of 3.2–3.7 ppm. Although, as noted earlier, this genus can

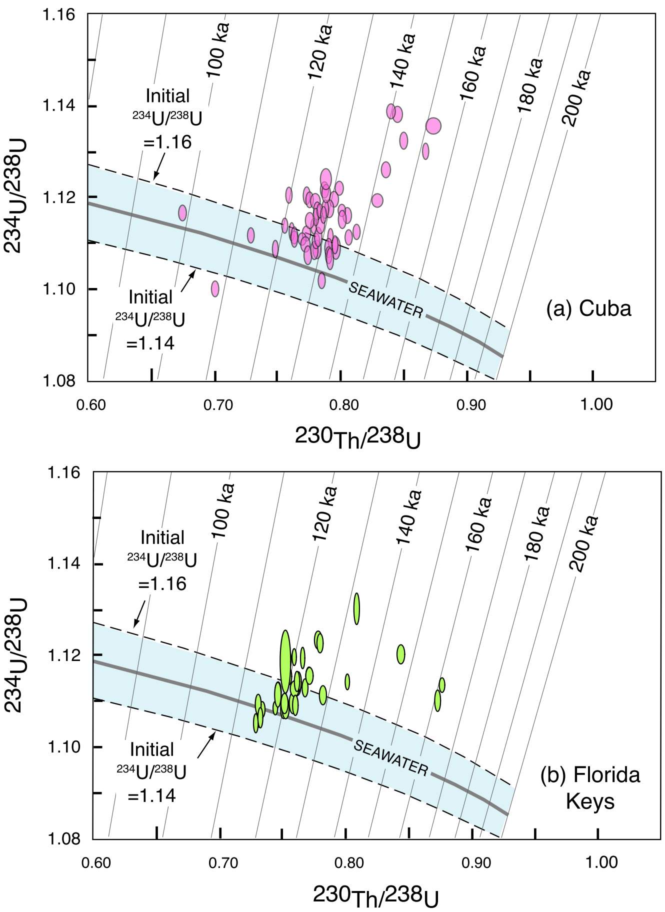

Fig. 9. Isotopic evolution diagrams (drawn using software in Ludwig, 2001) of (a) corals from the Jaimanitas Formation at Guantanamo Bay (this study) and (b) corals from the Key Largo Limestone of the Florida Keys (from Muhs et al., 2011). Ellipses show 2-sigma uncertainties in isotopic activity ratios. Bold solid line shows theoretical isotopic evolution pathway for a coral with an initial $^{234}U/^{238}U$ activity value of 1.15 (modern mean seawater value) and a closed-system history; dashed lines show similar pathways for corals with initial $^{234}U/^{238}U$ values of 1.16 and 1.14, values that bound the range of variability of modern seawater. Not included in figure are samples that have evidence of bulk U loss or gain (see Table 1).

sometimes have U contents this high, we note that neither the fossil *Siderastrea* higher in this section nor the modern *Siderastrea* at Cable Beach have U contents as high as these lower in the section. Hence, we suspect that these samples have acquired secondary addition of bulk U sometime after emergence and such additions would explain the younger apparent ages if the corals were of last-interglacial age. Furthermore, two of these corals (Cuba 7-5 and 7-6) have initial $^{234}U/^{238}U$ values that are *lower* than what is found in modern seawater. Both Cuba 7-7 and 7-8, found below the problematic *Siderastrea* specimens, have U contents that fall within the range of values reported for modern *Orbicella* and *Diploria*. Nevertheless, because these two corals are physically close to the problematic samples, we also consider Cuba 7-7 and 7-8 to be suspect and do not include them in our interpretations.

The roadcut exposure in the inner part of the reef exposed on Marine Hill also shows problems with likely U additions. Cuba 8-1, 8-2, and 8-4 are *Orbicella* and *Siderastrea* that have U contents above 3 ppm, higher than their modern equivalents that we analyzed (Table 1). Although Cuba 8-4 gives an age that is consistent with those for corals at Pier C, Hospital Cay, Cable Beach, and the other localities, both Cuba 8-1 and 8-2 give younger-than-expected ages, again suggesting secondary U additions. Cuba 8-3A, an *Acropora cervicornis* specimen from this section, shows the most obvious example of secondary U addition, with a U content of ~9 ppm and a much younger-than-expected age. An analysis from a different part of this coral gave different results, but also yielded a high U content (~7 ppm) and again a younger-than-expected age. Different initial $^{234}U/^{238}U$ values (one lower than modern seawater) as well as different measured $^{230}Th/^{238}U$ values in these two subsamples indicate that the secondary U addition process in this sample is complex. We therefore reject all apparent ages from this outcrop.

Finally, poor results were also obtained from most of the corals sampled in the exposed, outer-reef facies cliff section at Chapman Beach. U contents above 4 ppm, higher than in modern corals, were measured in *Acropora palmata* specimens Cuba 31-3 and 31-8. Apparent ages of these corals are significantly younger than those from the other parts of Guantanamo Bay. Cuba 31-4, also an *Acropora palmata* specimen, gave a U content of 3.7 ppm, within the range of modern corals of this genus (Cross and Cross, 1983), but this sample also gave an initial $^{234}U/^{238}U$ value *below* that of modern seawater. Cuba 31-11, an *Orbicella*, gave a U content of 3.34 ppm, which is too high for this genus (Table 1). Two of the other corals sampled at this section, Cuba 31-5 and 31-10 (as well as Cuba 31-11), have initial $^{234}U/^{238}U$ values greater than 1.20, well above the range of modern seawater. Only two samples (Cuba 31-6 at 5.5 m depth and Cuba 31-1, at 7.2 m depth), both *Acropora palmata* colonies in growth position, yielded acceptable U contents, high $^{230}Th/^{232}Th$ values, and initial $^{234}U/^{238}U$ values that, while higher than modern seawater, are not excessively high. These two corals gave apparent ages of ~120 ka and ~125 ka. Because of the variable and complex evidence for open-system conditions at Chapman Beach, we reject all other apparent ages of corals from this section.

3.3. Open-system uranium-series ages

As discussed earlier, Gallup et al. (1994) pointed out that corals with elevated initial $^{234}U/^{238}U$ values from within the same reef terrace tend to yield older apparent ages and other studies have borne out this interpretation. Thompson et al. (2003), following on the observations of Gallup et al. (1994), devised a scheme for correcting apparent older-aged corals that have elevated initial $^{234}U/^{238}U$ activity values. This method, applied to corals on Barbados (Muhs and Simmons, 2017; Thompson and Goldstein, 2005), the Bahamas (Thompson et al., 2011), and Australia (O'Leary et al., 2013) appears to yield geologically reasonable "corrected" open-system ages. It is likely that the variables affecting open-system behavior in corals include lithology, hydrogeology, climate, and sedimentology, and will vary from region to region. Thus, the U-series geochronology community has not yet reached a consensus on whether a correction scheme such as that of Thompson et al. (2003) has universal validity. Nevertheless, here we present corrected open-system ages, using the method of Thompson et al. (2003), in order to show alternative interpretations of the coral ages. We limited our calculations to those samples that do not have evidence of bulk U additions or loss, do not have initial $^{234}U/^{238}U$ activity values in excess of 1.20, or have initial $^{234}U/^{238}U$ activity values below the range of modern seawater. We also note which samples have, by the criterion of Thompson et al. (2011), ^{232}Th concentrations that are above the threshold value (>0.0004 ppm) used by these investigators, indicating a potentially significant amount of inherited ^{230}Th.

Applying the Thompson et al. (2003) correction method to corals from Guantanamo Bay results in corrections (to *younger* ages) ranging from as little as a couple hundred years for Cuba 23-5A to as much as ~17 ka for Cuba 9-9 (Table 2). Open-system ages

Table 2
Back-calculated initial $^{234}U/^{238}U$ values, "conventional" uranium-series ages (from Table 1), and "open-system" ages calculated from method by Thompson et al. (2003); open-system ages in bold are samples with low (≤0.0004 ppm) ^{232}Th concentrations.

Sample and location	Genus or species	Depth below surface of exposure (m)	Calculated initial $^{234}U/^{238}U$	±	"Conventional" $^{230}Th/^{238}U$ age (ka)	±	"Open-system" $^{230}Th/^{238}U$ age (ka)	±	Other notes
PIER C, west-facing ditch exposure									
Cuba 9-1B	*Siderastrea* sp.	1.1	1.1577	0.0015	125.1	0.7	**120.7**	**1.0**	
Cuba 9-1C	*Siderastrea* sp.	1.3	1.1658	0.0022	127.1	0.7	**119.5**	**1.4**	
Cuba 9-1D	*Siderastrea* sp.	1.6	1.1699	0.0020	126.2	0.9	**116.9**	**1.3**	
Cuba 9-1E	*Siderastrea* sp.	1.7	1.1675	0.0018	127.4	0.6	**119.0**	**1.1**	
Cuba 9-1F	*Siderastrea* sp.	1.9	1.1574	0.0016	123.1	0.8	**118.9**	**1.1**	
Cuba 9-1H	*Siderastrea* sp.	2.7	1.1743	0.0019	127.8	0.8	116.7	1.3	High ^{232}Th
PIER C, east-facing road cut exposure									
Cuba 9-4a	*Siderastrea* sp.	2.6	1.1641	0.0022	128.5	0.9	121.6	1.5	High ^{232}Th
Cuba 9-4a rpt	*Siderastrea* sp.	2.6	1.1672	0.0021	128.8	0.6	120.4	1.3	High ^{232}Th
Cuba 9-4	*Siderastrea* sp.	2.6	1.1674	0.0022	127.2	0.7	**118.8**	**1.4**	
Cuba 9-5	*Siderastrea* sp.	3.2	1.1576	0.0025	123.1	0.8	118.7	1.5	High ^{232}Th
Cuba 9-6	*Siderastrea* sp.	3.7	1.1586	0.0019	128.4	0.8	**123.6**	**1.2**	
Cuba 9-7	*Siderastrea* sp.	4.0	1.1579	0.0024	132.0	0.9	**127.4**	**1.6**	
Cuba 9-8	*Orbicella nancyi*	4.3	1.1598	0.0019	120.4	0.6	115.2	1.1	High ^{232}Th
Cuba 9-9	*Orbicella nancyi*	4.7	1.1880	0.0020	142.0	1.0	**125.1**	**1.4**	
Cuba 9-11	*Orbicella annularis*	5.7	1.1779	0.0019	141.6	1.2	128.7	1.4	High ^{232}Th
Cuba 9-12	*Orbicella annularis*	5.8	1.1698	0.0020	134.8	0.9	**125.3**	**1.4**	
Cuba 9-13	*Montastraea cavernosa*	6.2	1.1660	0.0020	138.1	0.8	**130.1**	**1.3**	
Cuba 9-14	*Siderastrea* sp.	6.4	1.1537	0.0022	127.2	0.8	124.5	1.5	High ^{232}Th
Cuba 9-15	*Eusmilia fastigata*	6.6	1.1598	0.0019	125.8	0.9	120.6	1.2	High ^{232}Th
Cuba 9-16	*Siderastrea* sp.	6.8	1.1628	0.0019	127.1	0.7	120.6	1.2	High ^{232}Th
Cuba 9-17	*Porites* sp.	7.2	1.1549	0.0027	132.9	0.9	129.5	1.7	High ^{232}Th
PIER C, early exploratory samples									
Cuba 1	*Siderastrea sideria*	0–7	1.1742	0.0024	127.9	0.9	**116.8**	**1.5**	
Cuba 2	*Siderastrea sideria*	0–7	1.1780	0.0024	127.1	1.0	**114.6**	**1.5**	
Cuba 3	*Solenastrea bournoni*	0–7	1.1643	0.0019	125.5	0.8	**118.4**	**1.2**	
HOSPITAL CAY									
Cuba 29-1	*Colpophyllia* sp.	~4.5	1.1521	0.0020	119.4	0.6	**117.3**	**1.3**	
Cuba 29-2	*Orbicella nancyi*	~4.5	1.1727	0.0020	130.6	0.9	120.0	1.3	High ^{232}Th
Cuba 29-3	*Siderastrea* sp.	~4.5	1.1558	0.0022	128.5	0.9	**124.8**	**1.5**	
Cuba 29-4	*Colpophyllia* sp.	~4.5	1.1688	0.0022	128.9	0.7	**120.0**	**1.4**	
SOUTH OF SHERMAN AVENUE									
Cuba 14-A	*Siderastrea* sp.	~1.5	1.1633	0.0020	136.5	0.9	129.7	1.3	High ^{232}Th
Cuba 14-B	*Siderastrea* sp.	~1.5	1.1600	0.0024	128.8	0.8	123.4	1.5	High ^{232}Th
CABLE BEACH, main exposure									
Cuba 23-7	*Diploria* cf. *D. strigosa*	3.6	1.1611	0.0022	131.9	0.8	**126.0**	**1.5**	
Cuba 23-11	*Diploria* sp.	4.55	1.1679	0.0023	133.7	0.8	**125.0**	**1.5**	
Cuba 23-6	*Diploria* sp.	4.9	1.1589	0.0028	133.7	1.0	128.7	1.9	High ^{232}Th
Cuba 23-5	*Orbicella nancyi*	5.7	1.1996	0.0020	151.8	0.8	**129.8**	**1.4**	
Cuba 23-5A	*Diploria* sp.	5.9	1.1477	0.0019	132.2	0.8	**131.9**	**1.3**	
Cuba 23-4A	*Siderastrea* sp.	6.3	1.1764	0.0018	131.3	0.8	**119.2**	**1.2**	
Cuba 23-3	*Orbicella nancyi*	7.35	1.1992	0.0022	145.1	1.0	**123.6**	**1.5**	
Cuba 23-2	*Diploria* sp.	7.35	1.1558	0.0021	132.3	0.8	**128.7**	**1.4**	
Cuba 23-1	*Diploria* sp.	7.8	1.1597	0.0022	133.3	0.8	**128.0**	**1.5**	
CABLE BEACH, cliff exposure ~30 m to the north of main exposure									
Cuba 23-10	*Diploria* cf. *D. strigosa*		1.1567	0.0019	126.2	0.9	**122.1**	**1.3**	
MARINE HILL, outer part									
Cuba 7-2	*Porites* cf. *P. asteroides*	0.9	1.1704	0.0017	133.1	0.8	123.5	1.1	High ^{232}Th
Cuba 7-3A	*Siderastrea* sp.	0.8	1.1696	0.0021	129.9	0.9	**120.6**	**1.4**	
Cuba 7-3B	*Siderastrea* sp.	0.9	1.1700	0.0019	124.8	0.7	**115.5**	**1.2**	
Cuba 7-3C	*Siderastrea* sp.	1.0	1.1709	0.0022	124.0	0.7	**114.4**	**1.4**	
CHAPMAN BEACH									
Cuba 31-6	*Acropora palmata*	5.5	1.1688	0.0019	119.9	0.6	**111.2**	**1.2**	
Cuba 31-1	*Acropora palmata*	7.2	1.1564	0.0019	125.2	0.9	**121.3**	**1.2**	

for most corals are 5–10 ka younger than their apparent, uncorrected ages. Nevertheless, with one exception (Cuba 31-6 from Cable Beach, which is ~111 ka), open-system coral ages still fall within the range of what would be considered to be MIS 5.5. When we apply the Thompson et al. (2003) criterion for significant ^{232}Th concentrations (eliminating those with concentrations higher than ~0.0004 ppm), 31 samples remain. At Pier C, this additional culling results in somewhat better agreement of "corrected" open-system ages with stratigraphic position, particularly on the thick, east-facing roadcut exposure (Fig. 10). If these corrections are accepted, the open-system ages indicate that reef growth during the last interglacial period at Guantanamo Bay began sometime before ~130 ka and continued until sometime just after ~119 ka. At Cable Beach, open-system age calculations do not provide good agreement with the stratigraphic framework (Fig. 11). The most obvious reversal is with samples Cuba 23-3 (at the base of a large *Orbicella nancyi* colony), which gives an apparent open-system age of ~124 ka, and Cuba 23-5 (at the top of the same colony), which gives an apparent open-system age of ~130 ka. A similar situation occurs at outer Marine Hill, where a *Siderastrea* colony (Cuba 7-3A) gives a significantly older (open-system) age (~121 ka) than two colonies that are stratigraphically below it (~115-114 ka). Other open-system ages, particularly at Cable Beach, are more difficult to assess, because of the three-dimensional nature of a reef. Younger corals can colonize openings in an existing reef, potentially at positions deeper (and thus appearing to be stratigraphically older) than coral colonies that are already established.

3.4. Late Quaternary uplift rates

There are three requirements for calculation of an uplift rate from marine terrace data: (1) the age of the terrace; (2) the elevation of the terrace, specifically that part of it that best represents sea level at the time of formation; and (3) paleo-sea level at the time of terrace formation. Field and laboratory data presented here provide (1) and (2); studies of emergent terraces from tectonically stable areas provide (3). Commonly, paleo-sea level at the peak of the last interglacial period is thought to have been +2 to +10 m relative to present, based on early studies by Veeh (1966) on tectonically stable coastlines. Many researchers assume a rough average of +6 m and indeed some tectonically stable localities have last-interglacial sea level records remarkably close to this figure, such as Isla Guadalupe off Baja California and the Florida Keys (Muhs et al., 2002b, 2011). Nevertheless, it is now well established that glacial isostatic adjustment (GIA) processes will generate variations on this average eustatic value from coast to coast, depending on the physical geography of the continent or island, the extent of continental or insular shelves, the distance from former continental ice sheets, and other variables (Creveling et al., 2015; Lambeck et al., 2012).

In a recent study, Creveling et al. (2015) modeled the amount of departure of last interglacial sea-level elevations from purely eustatic values for a variety of localities around the world. In conducting this modeling, Creveling et al. (2015) considered eustatic values of both +6 m and +8 m, relative to present. These investigators also considered what departures in sea level elevations would be from purely eustatic values at both the start (taken to be ~127 ka) and end (taken to be ~120 ka) of the last interglacial period. At ~120 ka, departures from purely eustatic values of paleo-sea level could result in relative sea levels as high as +11–13 m above present (at localities close to North American ice sheets) to as little as +5–8 m above present (at Southern Hemisphere localities, distant from North American ice sheets). The areas closest to Guantanamo Bay, Cuba that were modeled in this study are Haiti and the Cayman Islands, where local, relative paleo-sea levels could have been +8–9 m above present (assuming eustatic values of +6 m) to +10–11 m above present (assuming eustatic values of +8 m) at the end of the of the last interglacial period. In order to

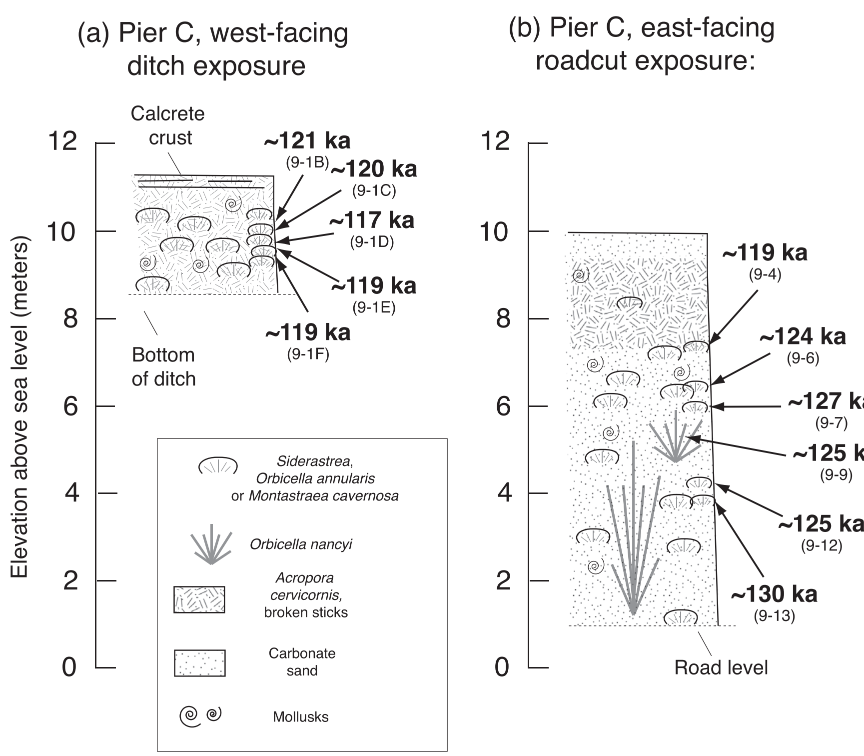

Fig. 10. Enlarged diagram of cliff sections at Pier C (see Fig. 7), with "corrected" open-system U-series ages using the correction scheme of Thompson et al. (2011); ages taken from Table 2. Not shown are "corrected" U-series ages of corals with ^{232}Th concentrations higher than 0.0004 ppm.

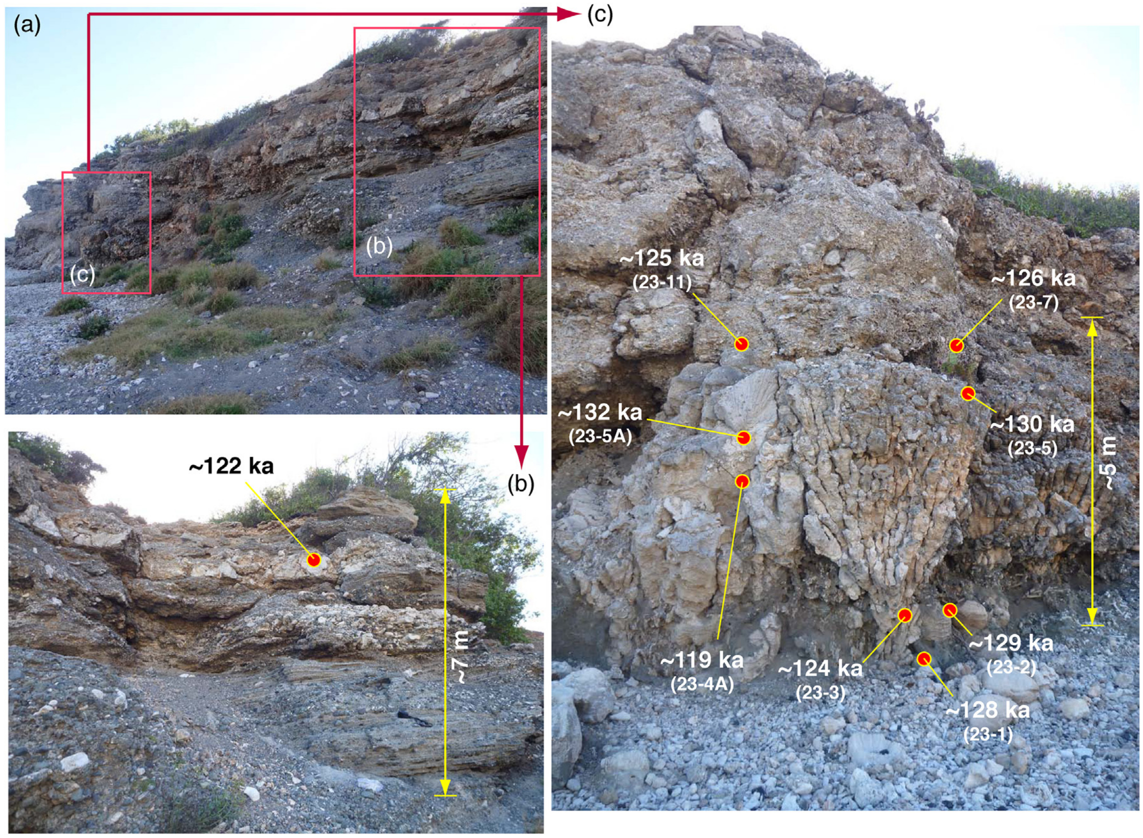

Fig. 11. Photographs showing cliff section exposed on the western side of Cable Beach (see Fig. 5a for general location shown in (a); (b) is close-up of landward part of exposure; (c) is close-up of same part of reef shown in Fig. 5b), with "corrected" open-system U-series ages using the correction scheme of Thompson et al. (2011); ages taken from Table 2. Not shown are "corrected" U-series ages of corals with ^{232}Th concentrations higher than 0.0004 ppm.

consider all possibilities, we calculated uplift rates using relative paleo-sea levels of +6, +8, +9, +10, and +11 m and last-interglacial *end* times of ~125 ka, ~120 ka, and 115 ka (Table 3). All three age estimates can be considered as possibilities, given both the "open-system" and "closed-system" age estimates in Table 2. In addition, we also considered paleo-sea levels modeled by Creveling et al. (2015), again using nearby Haiti and the Cayman Islands, at the *start* of the last interglacial period, considered by these workers to be ~127 ka. Sea levels at these times are modeled to be lower, ranging from +4.2 m to +7.5 m (Table 4).

It is important to note other criteria we used for calculation of uplift rates. As discussed earlier, we use the elevation data measured for four of our localities, Hospital Cay, Pier C, Cable Beach, and Chapman Beach (Fig. 8), with a +3-m adjustment for coral habitat depth (based on modern observations by Shinn et al. (1989)) added to the highest reef elevations at Hospital Cay, Pier C, and Chapman Beach (Table 3). This adjustment corresponds to the shallowest depths for optimum growth of coral taxa (*Orbicella annularis*, *Montastraea cavernosa*, *Siderastrea* sp., *Diploria* sp., and *Colpophyllia* sp.) that we analyzed from the highest elevations at these localities. Based on observations reported by Shinn et al. (1989), some of the coral species considered here have depth ranges that go deeper than this value (e.g., *Diploria strigosa*, optimum is 3–10 m, but maximum is ~40 m; *Siderastrea siderea*, optimum is 3–20 m, but maximum is ~70 m; *Orbicella annularis*, optimum is 3–45 m, but maximum is 80 m). If the corals we examined had been living at these greater possible depths, our calculated uplift rates would be too low. This is unlikely, however, because if the corals we studied were growing in water tens of meters below sea level, it is likely that we would have also observed marine deposits inland of those studied, at higher elevations, that had grown at shallower depths.

Results indicate that under virtually any scenario, uplift rates in the Guantanamo Bay area are fairly low (Tables 3 and 4). In all cases considered, late Quaternary uplift rates are 0.11 m/ka or less and under some scenarios, less than a third of this value. Nevertheless, it is also clear from the results that some measureable amount of uplift has occurred at Guantanamo Bay since the last interglacial period, even using the most liberal estimates (+11 m) of paleo-sea level. An interpretation of uplift under any estimate of last-interglacial paleo-sea level would be incorrect, however, if we modify our assumption of a minimum +3 m coral habitat water depth adjustment to greater depths, as discussed above. However, several of our exposed, outer-coast localities (Fisherman Point, the Lighthouse, Cable Beach, and Windmill Beach) and one other (the "South of Sherman Avenue locality") have inner edge elevations that fall very close to the same elevations as our (minimally) corrected lagoonal facies deposits (Fig. 8). Therefore, while all possible uplift rates calculated are rather low, we do consider that there has been measurable late Quaternary uplift at Guantanamo Bay since the end of the last interglacial period.

4. Discussion

4.1. Geomorphology, stratigraphy, and coral ages at Guantanamo Bay

With the exception of a small, isolated fragment of ancient reef at ~40 m elevation, there is no geomorphic evidence of more than one reef terrace in the Guantanamo Bay area. Indeed, the

Table 3
Calculations of alternative late Quaternary tectonic uplift rates, Guantanamo Bay, Cuba: end of the last interglacial period.

Locality	Measured elevation (m)[a]	Facies	Corrected elevation (m)[b]	Paleo-sea level (m)[c]	Amount of uplift (m)	Age (ka)	Uplift rate (m/ka)
Hospital Cay	10.8	Lagoonal	13.8	6	7.8	125	0.062
	10.8		13.8	8	5.8	125	0.046
	10.8		13.8	9	4.8	125	0.038
	10.8		13.8	10	3.8	125	0.030
	10.8		13.8	11	2.8	125	0.022
	10.8		13.8	6	7.8	120	0.065
	10.8		13.8	8	5.8	120	0.048
	10.8		13.8	9	4.8	120	0.040
	10.8		13.8	10	3.8	120	0.032
	10.8		13.8	11	2.8	120	0.023
	10.8		13.8	6	7.8	115	0.068
	10.8		13.8	8	5.8	115	0.050
	10.8		13.8	9	4.8	115	0.042
	10.8		13.8	10	3.8	115	0.033
	10.8		13.8	11	2.8	115	0.024
Pier C	11.4	Lagoonal	14.4	6	8.4	125	0.067
	11.4		14.4	8	6.4	125	0.051
	11.4		14.4	9	5.4	125	0.043
	11.4		14.4	10	4.4	125	0.035
	11.4		14.4	11	3.4	125	0.027
	11.4		14.4	6	8.4	120	0.070
	11.4		14.4	8	6.4	120	0.053
	11.4		14.4	9	5.4	120	0.045
	11.4		14.4	10	4.4	120	0.037
	11.4		14.4	11	3.4	120	0.028
	11.4		14.4	6	8.4	115	0.073
	11.4		14.4	8	6.4	115	0.056
	11.4		14.4	9	5.4	115	0.047
	11.4		14.4	10	4.4	115	0.038
	11.4		14.4	11	3.4	115	0.030
Cable Beach	14.3	Exposed outer coast	14.3	6	8.3	125	0.066
	14.3		14.3	8	6.3	125	0.050
	14.3		14.3	9	5.3	125	0.042
	14.3		14.3	10	4.3	125	0.034
	14.3		14.3	11	3.3	125	0.026
	14.3		14.3	6	8.3	120	0.069
	14.3		14.3	8	6.3	120	0.052
	14.3		14.3	9	5.3	120	0.044
	14.3		14.3	10	4.3	120	0.036
	14.3		14.3	11	3.3	120	0.028
	14.3		14.3	6	8.3	115	0.072
	14.3		14.3	8	6.3	115	0.055
	14.3		14.3	9	5.3	115	0.046
	14.3		14.3	10	4.3	115	0.037
	14.3		14.3	11	3.3	115	0.029
Chapman Beach	14.8	Exposed outer coast	17.8	6	11.8	125	0.094
	14.8		17.8	8	9.8	125	0.078
	14.8		17.8	9	8.8	125	0.070
	14.8		17.8	10	7.8	125	0.062
	14.8		17.8	11	6.8	125	0.054
	14.8		17.8	6	11.8	120	0.098
	14.8		17.8	8	9.8	120	0.082
	14.8		17.8	9	8.8	120	0.073
	14.8		17.8	10	7.8	120	0.065
	14.8		17.8	11	6.8	120	0.057
	14.8		17.8	6	11.8	115	0.103
	14.8		17.8	8	9.8	115	0.085
	14.8		17.8	9	8.8	115	0.076
	14.8		17.8	10	7.8	115	0.068
	14.8		17.8	11	6.8	115	0.059

[a] Highest elevation measured in the field at location given.
[b] Lagoonal facies localities and Chapman Beach given additional 3 m of paleo-sea level to account for minimum habitat depth.
[c] Paleo-sea level above present estimated from minimum eustatic component (6 m) and range of GIA-adjusted sea-level estimates from Haiti and Cayman Islands at the end of the last interglacial period (Creveling et al., 2015).

Table 4
Calculations of alternative late Quaternary tectonic uplift rates, Guantanamo Bay, Cuba: start of the last interglacial period.

Locality	Measured elevation (m)[a]	Facies	Corrected elevation (m)[b]	Paleo-sea level (m)[c]	Amount of uplift (m)	Age (ka)	Uplift rate (m/ka)
Hospital Cay	10.8	Lagoonal	13.8	4.2	9.6	127	0.076
	10.8		13.8	5.5	8.3	127	0.065
	10.8		13.8	6.2	7.6	127	0.060
	10.8		13.8	7.5	6.3	127	0.050
Pier C	11.4	Lagoonal	14.4	4.2	10.2	127	0.080
	11.4		14.4	5.5	8.9	127	0.070
	11.4		14.4	6.2	8.2	127	0.065
	11.4		14.4	7.5	6.9	127	0.054
Cable Beach	14.3	Exposed outer coast	14.3	4.2	10.1	127	0.080
	14.3		14.3	5.5	8.8	127	0.069
	14.3		14.3	6.2	8.1	127	0.064
	14.3		14.3	7.5	6.8	127	0.054
Chapman Beach	14.8	Exposed outer coast	17.8	4.2	13.6	127	0.107
	14.8		17.8	5.5	12.3	127	0.097
	14.8		17.8	6.2	11.6	127	0.091
	14.8		17.8	7.5	10.3	127	0.081

[a] Highest elevation measured in the field at location given.
[b] Lagoonal facies localities and Chapman Beach given additional 3 m of paleo-sea level to account for minimum habitat depth.
[c] Paleo-sea level above present estimated from two possible eustatic components (6 m and 8 m) and range of GIA-adjusted sea-level estimates from Haiti and Cayman Islands at the start of the last interglacial period at 127 ka (Creveling et al., 2015).

overwhelming geomorphic evidence, from both the appearance in the field (Figs. 4a and 5a) and from elevation measurements (Fig. 8) is that the bay is rimmed by a single terrace landform. Examination of the hills surrounding the bay, at elevations above this fossil reef, did not reveal any evidence of a higher terrace nor did we find detrital corals lying on bedrock surfaces above the last interglacial reef. Further, there is no evidence of any lower-elevation terraces.

Within exposures around the bay and the outer coast, which are numerous (Fig. 3), we did not observe any stratigraphic evidence of more than one high sea stand. Growth-position corals are commonly observed in these exposures, and appear to represent a reef that experienced more-or-less continuous upward growth without interruption during a single high-sea stand. We specifically looked for evidence of either subaerial exposure (paleosols, karst surfaces, laminar calcretes) or erosion (wave-cut benches), but found no such evidence in any exposure examined.

Early workers on Barbados mapped and described only a single reef terrace marking the peak of the last interglacial period, equivalent to MIS 5.5 (Bender et al., 1979; Broecker et al., 1968; Mesolella et al., 1969; Taylor and Mann, 1991). Later workers described as many as three separate terraces dating to MIS 5.5 (Schellmann and Radtke, 2004; Speed and Cheng, 2004). One could argue that on an island such as Barbados, which has experienced significant long-term uplift, small variations in sea level within an interglacial period, if they indeed occurred, in principle could be resolved in the geomorphic record of reef terraces. This is possible because relatively rapid uplift could move a terrace out of erosional reach of a subsequent high-sea stand. Following on this concept, it could also be argued that on a coast with a low uplift rate or one that is tectonically stable, two or more separate high-sea stands within an interglacial could easily be blurred into a single landform through erosion of the earlier high stand or stands by the latest high stand. Yet, Thompson et al. (2011), following on the earlier work of Chen et al. (1991), White et al. (1998), and Wilson et al. (1998), propose that at least two high-sea stands occurred within the last interglacial period, as recorded on the tectonically stable islands of the Bahamas. By this line of reasoning, such a record could be present at Guantanamo Bay. Nevertheless, we observed no such evidence in our studies. Other islands in the region, such as the tectonically stable Florida Keys and the slowly uplifting island of Curaçao (Muhs et al., 2011, 2012a), also offer no evidence of more than one high-sea stand within the last interglacial period. Resolution of this issue is important, however, as sea level fluctuations within an interglacial period, of a magnitude of several meters, would require significant ice sheet growth during a time when Northern Hemisphere summer insolation was high (Berger and Loutre, 1991; Otto-Bliesner et al., 2006; Overpeck et al., 2006).

On the other hand, it is possible that GIA processes in near-field or intermediate-field localities might preclude field recognition of two high-sea stands within the last interglacial period. Dutton and Lambeck (2012) modeled relative sea level during the last interglacial period for a variety of localities worldwide. These simulations demonstrate that some far-field localities, such as Australia, may have had a relative sea level that was high early in the last interglacial period, followed by a gradually falling sea level. In contrast, near-field localities of the Caribbean and western Atlantic, such as Bermuda, the Bahamas and Haiti, closer to North American ice sheets, may have had a relative sea level that was low in the early part of the last interglacial period, followed by a rapid rise to a maximum value very late in the same period. Given its location, Cuba's coastline likely would have experienced a relative sea level history similar to those of the Bahamas and Haiti. Thus, if there were a second, eustatic sea-level high-sea stand during the latter part of the last interglacial period, it would have been superimposed on the rising maximum sea level controlled by GIA processes at this time and a record of such an event may not be apparent in the field.

4.2. Uplift rates at Guantanamo Bay and in the Caribbean region

Using a range of options for age and paleo-sea level for four different localities around Guantanamo Bay, it can be concluded that uplift rates in this part of Cuba have been modest since the last interglacial period. Calculated uplift rates, while measurable, range from only 0.02–0.11 m/ka, supporting the concept that motion today along the Oriente fault is dominantly horizontal, accommodating much of the movement along the North America-Caribbean plate boundary. Although Rojas-Agramonte et al. (2005)

hypothesized that uplift rates might be relatively high in the Santiago area (see earlier discussion), they also proposed that movement along the North America-Caribbean plate boundary since the Pliocene is transpressive, i.e., dominantly but not exclusively horizontal. Late Quaternary uplift rates in the range calculated here for Guantanamo Bay are similar to those in other regions characterized dominantly by strike-slip tectonics, such as much of the California coast west of the San Andreas Fault (see review by Muhs et al., 2014b). Uplift rates in coastal California are generally less than 0.5 m/ka and many localities have uplift rates that are less than 0.2 m/ka. Exceptions to this include areas adjacent to restraining bends in faults, such as that near the Palos Verdes Hills fault, where late Quaternary uplift rates are as high as ~0.7 m/ka, or seaward of the "Big Bend" area of the San Andreas Fault, where uplift rates are as high as ~5.0 m/ka.

In order to put the uplift rates reported here into a regional context, we compiled data to calculate late Quaternary uplift rates based on emergent reef terraces from around the Caribbean. In this compilation, we included only those localities where mapped terraces are found with good elevation data and reliable U-series ages on corals date the terraces to the last interglacial period. Following Creveling et al. (2015), we chose an age of ~120 ka as the time of termination of the last interglacial period. Because the Caribbean and western Atlantic region spans a considerable latitudinal extent, local sea level elevations during the last interglacial period will vary due to GIA effects, combined with the eustatic component (Creveling et al., 2015; Lambeck et al., 2012). As discussed earlier, Creveling et al. (2015) modeled GIA effects for much of the region for both the beginning (~127 ka) and end (~120 ka) of the last interglacial period, as well as considering two estimates of the eustatic component of sea level (+6 m and +8 m of sea-level equivalent). For the end of the last interglacial period, at ~120 ka, this results in local sea levels, including both the eustatic and GIA-modeled components, being as high as ~11 m or as low as ~6 m above sea level. We computed uplift rates for the region using both of these local paleo-sea level estimates.

It is apparent from this compilation that uplift rates in excess of 0.1 m/ka are rare in the Caribbean region (Fig. 12). Most areas are either tectonically stable or uplifting very slowly. There are a few areas where uplift rates exceed 0.1 m/ka, however. Barbados has a last-interglacial reef crest that ranges in elevation from ~15 m to ~61 m (Taylor and Mann, 1991). Thus, considering paleo-sea levels as low as +6 m and as high as +11 m results in a range of uplift rates on this island from 0.03 to 0.46 m/ka. Taylor and Mann (1991) attributed variability in uplift rates on Barbados to local structures (folds) because of active shortening on this accretionary prism. Over much of northern Jamaica, what has been mapped as the Falmouth Formation (Henry, 1978a, 1978b) corresponds to what is likely the last interglacial reef terrace (Moore and Somayajulu, 1974; Szabo, 1979). In most places, the elevation of this terrace is only a few meters above sea level, but in the Oracabessa area (Fig. 2), it attains an elevation of ~15 m (Cant, 1970, 1973). We hypothesize that the higher elevation of the Falmouth Formation here is due to uplift derived from a restraining bend in the fault that borders the northern shore of Jamaica (Figs. 1 and 2), but this requires additional testing with detailed elevation measurements and better geochronology. Haiti shows a range of uplift rates similar to Barbados, and like Barbados, the areas with the highest uplift rates are those coinciding with the axial traces of folds (Mann et al., 1995). These areas of active folding could, in turn, be a function of compression due to proximity of the areas to restraining bends in a fault that borders the northwestern part of Haiti (Fig. 12) and continues as the Oriente fault farther west (Fig. 2). Uplift of the northwestern coast of Haiti has been a long-term geologic process, demonstrated by the number and elevation of reef terraces in that area. Almost a century ago, Woodring et al. (1924) pointed out that there are as many as 28 uplifted reef terraces on the northwestern coast of Haiti, rising to an elevation of at least ~430 m. In a later study, Dodge et al. (1983) reported terraces on this part of Haiti as high as ~600 m. Such terraces likely date back to the early Pleistocene and imply that crustal compression and uplift, generated by the restraining bend in the adjacent fault, has been an ongoing process for a long time.

Although our data show that the rate of uplift in the Guantanamo Bay region is modest, higher rates of uplift are likely for other parts of the eastern and southern Cuban coast. From the air, we have observed multiple reef terraces off the eastern coast of Cuba, rising to an elevation of up to ~400 m or more. The terraces are striking geomorphic features visible on satellite imagery (Fig. 13). To the best of our knowledge, these terraces have not been dated, but we hypothesize that the last interglacial terrace in this part of Cuba is at a significantly higher elevation than in the Guantanamo Bay area. In a reach of the southern coast of Cuba starting approximately 25 km to the west of Guantanamo Bay and continuing for an additional ~50 km to Santiago de Cuba (Fig. 2), examination of satellite imagery reveals the presence of perhaps five or six terraces, rising to elevations of at least ~100 m in places. Rojas-Agramonte et al. (2005) report terraces in this area as high as ~200 m, as discussed earlier. Still farther west, in the coastal region to the east of Cabo Cruz (Fig. 2), Taber (1934) reported multiple reef terraces. We have not observed these terraces personally, but examination of satellite imagery indicates there may be 10 or more terraces rising to elevations well over ~250 m. If these simple observations of what appears to be terrace geomorphology are correct, they imply higher rates of uplift than in our study area and suggest that the very low uplift rate around Guantanamo Bay actually may be anomalous for the southern coast of Cuba.

4.3. Implications for GIA models

What is also apparent from the compilation of uplift rates shown in Fig. 12 is that either many areas of the Caribbean and western Atlantic are subsiding or that some GIA-corrected paleo-sea level estimates generated by modeling are too high. For example, with GIA modeling, Lambeck et al. (2012) and Creveling et al. (2015) hypothesize that Bermuda had a last-interglacial sea level at 11–13 m above present, at the end of the high-sea stand. However, the highest undisputed last-interglacial deposits on Bermuda range from +5 m to +6 m (see summary in Vacher and Rowe, 1997, p. 78), and last-interglacial localities that we have measured ourselves on Bermuda range from ~1.5 m to ~7.7 m. If the GIA modeling is correct, it is possible that Bermuda has been subsiding since the last interglacial period. Farther south, GIA-based estimates of last-interglacial paleo-sea level range from +9 to 11 m for the northern Caribbean and adjacent western Atlantic to +7–9 m for the southern Caribbean (Creveling et al., 2015; Lambeck et al., 2012). The implication of this is that a last-interglacial shoreline lower than +7 m on any Caribbean island or continental coastline must have subsided since the end of the last interglacial period. Based on reported maximum elevations of reef terraces, this would imply that most of the Florida Keys, many Bahamas islands, northern Cuba, the Yucatan Peninsula, the Cayman Islands, much of the northern coast of Jamaica, Isla Mona off Puerto Rico, Gonave Island off Haiti, and most of Puerto Rico's western coast have all subsided in the past 120,000 years (Fig. 12). Given the diverse geologic settings of these various islands and continental coastlines, some of which are in tectonically stable regions and others that are adjacent to major faults or even plate boundaries, this does not seem very likely. It is difficult to imagine what geologic process could bring about subsidence of several

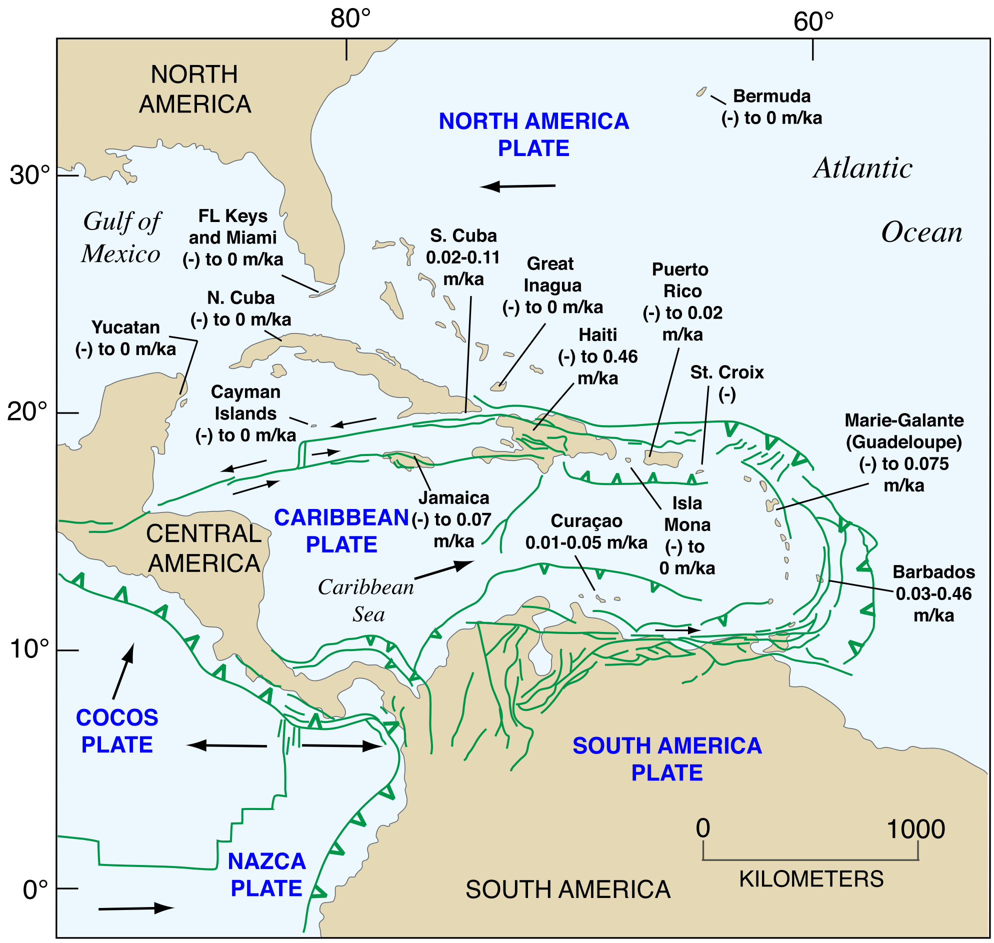

Fig. 12. Tectonic map of the Caribbean Basin and surrounding areas (sources as in Fig. 1), with late Quaternary uplift rates, based on elevations of the ~120 ka reef terrace. Paleo-sea level data, taken as +6 m to +11 m, are taken from Creveling et al. (2015). A minus sign in parentheses "(–)" indicates late Quaternary subsidence using these paleo-sea level estimates. Sources of elevation and age data: Bermuda, Harmon et al. (1983), Vacher and Rowe (1997), and Muhs et al. (2002a); Florida Keys and Miami, Muhs et al. (2011); northern Cuba, Toscano et al. (1999); Yucatan, Szabo et al. (1978) and Blanchon et al. (2009); Cayman Islands, Woodroffe et al. (1983); Jamaica, Cant (1970, 1973), Moore and Somayajulu (1974), and Szabo (1979); southern Cuba, this study; Great Inagua Island, Chen et al. (1991) and Thompson et al. (2011); Haiti, Dodge et al. (1983), Hamelin et al. (1991), Mann et al. (1995), and Dumas et al. (2006); Isla Mona, Winter et al. (2003); Puerto Rico, Taggart and Joyce (1990); St. Croix, Toscano et al. (2012); Barbados, Taylor and Mann (1991), Gallup et al. (1994, 2002), Edwards et al. (1997), and Speed and Cheng (2004); Marie-Galante Island (Guadeloupe islands), Feuillet et al. (2004); Curaçao, Muhs et al. (2012a).

meters over the past ~120,000 years over a large region with such tectonic complexity. One exception to this is the island of St. Croix, where the last interglacial reef is about 9.5 m below sea level, based on coring and dating reported by Toscano et al. (2012). For this island, it is difficult to explain the position of the last interglacial reef by any process other than subsidence. For all the other localities around the region, however, the simplest explanation is that some of the GIA-modeled estimates of paleo-sea level reported by Lambeck et al. (2012) and Creveling et al. (2015) are too high and require revision of the boundary conditions of the models.

The results presented here do support some other aspects of GIA modeling, however. Based on the low uplift rates reported here, coral reefs dating to the ~100 ka (MIS 5.3) or ~80 ka (MIS 5.1) sea stands should not be emergent in the Guantanamo Bay area. The GIA modeling of Potter and Lambeck (2003) indicates that on tectonically stable Bermuda and the U.S. Atlantic Coastal Plain, 80 ka marine deposits should be emergent. Field and laboratory studies indicate that this is in fact the case (Muhs et al., 2002a; Wehmiller et al., 2004). Potter and Lambeck's (2003) modeling also indicates that at ~80 ka, paleo-sea level in southern Cuba could have been ~12 m below present. If the uplift rates reported here (0.02–0.11 m/ka) are correct, then an ~80 ka reef terrace should have experienced only ~1.6–~8.2 m of uplift. With a paleo-sea level at ~12 m below present, this reef should still be submerged off of Guantanamo Bay. Based on our observations and dating, the lack of any evidence of a reef younger than ~120 ka at Guantanamo Bay supports the GIA modeling.

5. Conclusions

There has been considerable interest in the nature of the North America-Caribbean plate boundary along the northern margin of the Caribbean region. Previous investigators have suggested that the nature of the plate boundary in this area has evolved over time, but has been dominated by a transpressive regime since about the Pliocene. If so, we hypothesized that there should be at least a small, but measurable component of vertical movement in this part of southern Cuba. Guantanamo Bay, Cuba is situated in this area. We studied a number of sections exposing an unusually well preserved emergent reef terrace around Guantanamo Bay to determine its stratigraphy, elevation range, and age. An inner, protected, lagoonal facies of reef sediments is recognized, with abundant corals in growth position and elevations as high as ~11–12 m. An exposed, outer-coast reef facies is also recognized, with wave-cut benches in places as well as other species of corals in growth position; inner edges of outer-coast facies deposits are as high as ~14 m. Sixty-five

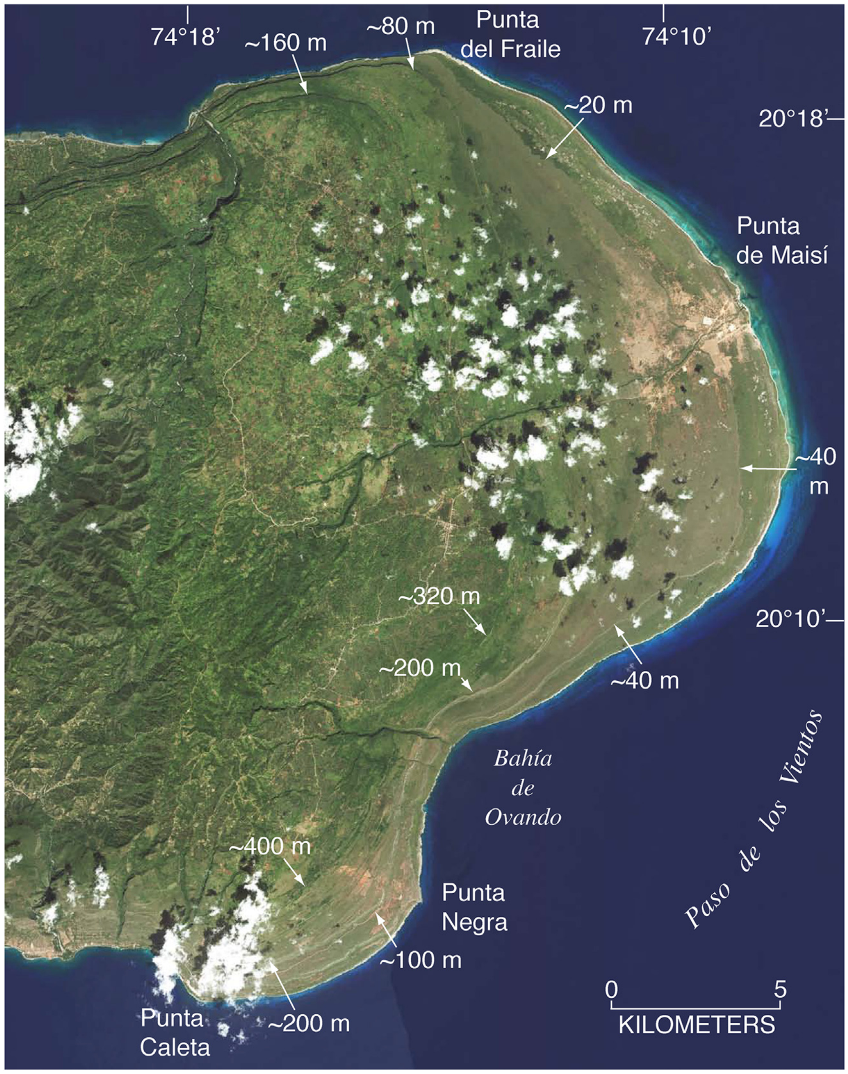

Fig. 13. World View 2 satellite image of Punta Caleta-Punta Negra-Punta de Maisí-Punta del Fraile area, eastern Cuba (see Fig. 2 for location), acquired on 20 February 2012, showing multiple emergent marine terraces rising to at least ~400 m. Arrows point to terrace outer edges; elevations are from 1:100,000-scale topographic maps with a contour interval of 40 m. Satellite image used courtesy of Digital Globe.

uranium-series analyses of unrecrystallized corals from six localities were generated. Some of these specimens show secondary additions of U, some show inheritance of Th, and others show elevated initial $^{234}U/^{238}U$ values. Nevertheless, about a dozen corals do not have these characteristics and have U-series ages ranging from ~133 ka to ~119 ka. Use of an open-system "correction" scheme yields a larger suite of coral age estimates, but the range of ages is similar, from ~130 ka to ~119 ka. Thus, by either method, ages of corals correlate this reef to the peak of the last interglacial period, MIS 5.5. Neither stratigraphic data nor U-series ages support the idea, reported from other localities, that there were two separate high stands of sea during MIS 5.5. Using estimates of paleo-sea level during MIS 5.5 (+6 to +11 m) and possible ages (~125 ka to ~115 ka) yields a range of late Quaternary uplift rates of 0.02–0.11 m/ka for the Guantanamo Bay area. This range of estimates supports the hypothesis that the tectonic uplift rate is low adjacent to the Oriente fault of this part of the North America-Caribbean plate boundary. Nevertheless, in areas of eastern and southern Cuba, to the east and west of Guantanamo Bay, aerial views and examination of satellite imagery show that there are multiple terraces, some rising to more than ~100 m (west of Guantanamo Bay) and ~400 m (east of Guantanamo Bay). In these areas, we hypothesize that there is a greater vertical component of movement and the low uplift rate at Guantanamo Bay itself may be something of an anomaly for this part of Cuba.

Using published data from other Caribbean islands and continental coastlines, we show that with the exception of Haiti and Barbados, uplift rates are low or zero on most insular and continental coastlines of the Caribbean region and adjacent parts of the western Atlantic. We note, however, that some recently published paleo-sea level estimates for the Caribbean region that account for GIA processes may be too high. Use of the upper ranges of these estimates would imply that many islands and continental coastlines have subsided since the close of the last interglacial period, a scenario that we consider unlikely over such a vast and tectonically diverse region. Nevertheless, our data support other aspects of GIA modeling. Given the low uplift rates reported here combined with estimated paleo-sea level (modeled for GIA effects), there should be no evidence of emergent ~80 ka marine deposits at Guantanamo Bay, in contrast to localities farther north, such as Bermuda and the U.S. Atlantic Coastal Plain. Our field and laboratory data indicate that there is no emergent reef around Guantanamo Bay that is younger than ~120 ka, which supports the GIA modeling.

Acknowledgments

This study was supported by the Climate and Land Use Change Research and Development Program of the U.S. Geological Survey (USGS) and is a contribution to the "Geologic records of high sea levels" project (http://gec.cr.usgs.gov/projects/sealevels/). It is a pleasure to thank the many people who helped us. First and foremost, we thank Michael R. McCord (former Environmental Director, U.S. Naval Base Guantanamo Bay, Cuba), who arranged our trips, provided logistical support, and gave us much encouragement for doing the study. We also wish to thank Mark Gettel (Environmental Office, U.S. Naval Base Guantanamo Bay, Cuba), who also provided logistical support; Gary Skipp (USGS), who X-rayed all the corals; Randy Schumann (USGS), who post-processed the GPS data; and Darren Van Sistine (USGS), who georeferenced Meinzer's geologic map of the area and provided the satellite image shown in Fig. 13. We thank Digital Globe for allowing use of the satellite image in Fig. 13. Margaret Berry and Janet Slate, both of the USGS, made very helpful comments on an earlier version of the paper, as did two anonymous QSR reviewers; thanks to all for these efforts. Any use of trade, product, or firm names is for descriptive purposes only and does not imply endorsement by the U.S. Government.

References

Academia de Ciencias de Cuba, Instituto de Geología y Paleontología, 1988. Mapa Geológico de Cuba, 40 sheets, scale, 1: 250,000.
Agassiz, A., 1894. A reconnoissance [sic] of the Bahamas and of the elevated reefs of Cuba in the steam yacht "Wild Duck," January to April, 1893. Bull. Mus. Comp. Zoology 26, 1–203.
Bard, E., Hamelin, B., Fairbanks, R.G., Zindler, A., 1990. Calibration of the ^{14}C timescale over the past 30,000 years using mass spectrometric U-Th ages from Barbados corals. Nature 345, 405–410.
Bender, M.L., Fairbanks, R.G., Taylor, F.W., Matthews, R.K., Goddard, J.G., Broecker, W.S., 1979. Uranium-series dating of the Pleistocene reef tracts of Barbados, west Indies. Geol. Soc. Am. Bull. Part I 90, 577–594.
Berger, A., Loutre, M.F., 1991. Insolation values for the climate of the last 10 million years. Quat. Sci. Rev. 10, 297–317.
Blanchon, P., Eisenhauer, A., Fietzke, J., Liebetrau, V., 2009. Rapid sea-level rise and reef back-stepping at the close of the last interglacial highstand. Nature 458, 881–885.
Bloom, A.L., Broecker, W.S., Chappell, J.M.A., Matthews, R.K., Mesolella, K.J., 1974. Quaternary sea level fluctuations on a tectonic coast: new ^{230}Th/^{234}U dates from the Huon Peninsula, New Guinea. Quat. Res. 4, 185–205.
Broecker, W.S., Thurber, D.L., 1965. Uranium-series dating of corals and oolites from Bahaman and Florida Key limestones. Science 149, 58–60.
Broecker, W.S., Thurber, D.L., Goddard, J., Ku, T.-L., Matthews, R.K., Mesolella, K.J., 1968. Milankovitch hypothesis supported by precise dating of coral reefs and deep-sea sediments. Science 159, 297–300.
Budd, A.F., Stemann, T.A., Johnson, K.G., 1994. Stratigraphic distributions of genera and species of Neogene to Recent Caribbean reef corals. J. Paleontology 68, 951–977.
Budd, A.F., Fukami, H., Smith, N.D., Knowlton, N., 2012. Taxonomic classification of the reef coral family Mussidae (Cnidaria: Anthozoa: Scleractinia). Zoological J. Linn. Soc. 166, 465–529.
Cabrera, M., Peñalver, L.L., 2001. Contribución a la estratigrafía de los depósitos cuaternarios de Cuba. Rev. Cuaternario Geomorfol. 15, 37–49.
Calais, E., Perrot, J., Mercier de Lépinay, B., 1998. Strike-slip tectonics and seismicity along the northern Caribbean plate boundary from Cuba to Hispaniola. Geol. Soc. Am. Special Pap. 326, 125–141.
Cant, R.V., 1970. Pleistocene Terraces Near Oracabessa. in: International Field Institute Guidebook to the Caribbean Island-arc System. American Geological Institute, Washington, D.C., pp. 40–43
Cant, R.V., 1973. Jamaica's Pleistocene reef terraces. Geol. Mijnb. 52, 157–160.
Chen, J.H., Edwards, R.L., Wasserburg, G.J., 1986. ^{238}U, ^{234}U, and ^{232}Th in seawater. Earth Planet. Sci. Lett. 80, 241–251.
Chen, J.H., Curran, H.A., White, B., Wasserburg, G.J., 1991. Precise chronology of the last interglacial period: ^{234}U-^{230}Th data from fossil coral reefs in the Bahamas. Geol. Soc. Am. Bull. 103, 82–97.
Cheng, H., Edwards, R.L., Shen, C.-C., Polyak, V.J., Asmerom, Y., Woodhead, J., Hellstrom, J., Wang, Y., Kong, X., Spötl, C., Wang, X., Alexander Jr., E.C., 2013. Improvements in ^{230}Th dating, ^{230}Th and ^{234}U half-life values, and U-Th isotopic measurements by multi-collector inductively coupled plasma mass spectrometry. Earth Planet. Sci. Lett. 371–372, 82–91.
Clark, P.U., Huybers, P., 2009. Interglacial and future sea level. Nature 462, 856–857.
Creveling, J.R., Mitrovica, J.X., Hay, C.C., Austermann, J., Kopp, R.E., 2015. Revisiting tectonic corrections applied to Pleistocene sea-level highstands. Quat. Sci. Rev. 111, 72–80.
Crosby, W.O., 1882. On the elevated coral reefs of Cuba. Proc. Boston Soc. Nat. Hist. 124–130, 22. .
Cross, T.S., Cross, B.W., 1983. U, Sr, and Mg in Holocene and Pleistocene corals *A. palmata* and *M. annularis*. J. Sediment. Petrology 53, 587–594.
Cutler, K.B., Edwards, R.L., Taylor, F.W., Cheng, H., Adkins, A., Gallup, C.D., Cutler, P.M., Burr, G.S., Bloom, A.L., 2003. Rapid sea-level fall and deep-ocean temperature change since the last interglacial period. Earth Planet. Sci. Lett. 206, 253–271.
Darwin, C., 1889. The Structure and Distribution of Coral Reefs, third ed. Smith, Elder & Co, London, p. 344.
Delanghe, D., Bard, E., Hamelin, B., 2002. New TIMS constraints on the uranium-238 and uranium-234 in seawaters from the main ocean basins and the Mediterranean Sea. Mar. Chem. 80, 79–93.
Dodge, R.E., Fairbanks, R.G., Benninger, L.K., Maurrasse, F., 1983. Pleistocene sea levels from raised coral reefs of Haiti. Science 219, 1423–1425.
Dumas, B., Hoange, C.T., Raffy, J., 2006. Record of MIS 5 sea-level highstands based on U/Th dated coral terraces of Haiti. Quat. Int. 145–146, 106–118.
Dutton, A., Lambeck, K., 2012. Ice volume and sea level during the last interglacial. Science 337, 216–219.
Dutton, A., Webster, J.M., Zwartz, D., Lambeck, K., Wohlfarth, B., 2015. Tropical tales of polar ice: evidence of Last Interglacial polar ice sheet retreat recorded by fossil reefs of the granitic Seychelles islands. Quat. Sci. Rev. 107, 182–196.
Edwards, R.L., Cheng, H., Murrell, M.T., Goldstein, S.J., 1997. Protactinium-231 dating of carbonates by thermal ionization mass spectrometry: implications for Quaternary climate change. Science 276, 782–786.
Edwards, R.L., Gallup, C.D., Cheng, H., 2003. Uranium-series dating of marine and lacustrine carbonates. Rev. Mineralogy Geochem. 52, 363–405.
Esat, T.M., McCulloch, M.T., Chappell, J., Pillans, B., Omura, A., 1999. Rapid fluctuations in sea level recorded at Huon Peninsula during the penultimate deglaciation. Science 283, 197–201.
Feuillet, N., Tapponnier, P., Manighetti, I., Villemant, B., King, G.C.P., 2004. Differential uplift and tilt of Pleistocene reef platforms and Quaternary slip rate on the Morne-Piton normal fault (Guadeloupe, French West Indies). J. Geophys. Res. 109, B02404. https://doi.org/10.1029/2003JB002496.
Gallup, C.D., Edwards, R.L., Johnson, R.G., 1994. The timing of high sea levels over the past 200,000 years. Science 263, 796–800.
Gallup, C.D., Cheng, H., Taylor, F.W., Edwards, R.L., 2002. Direct determination of the timing of sea level change during Termination II. Science 295, 310–313.
Hamelin, B., Bard, E., Zindler, A., Fairbanks, R.G., 1991. ^{234}U/^{238}U mass spectrometry of corals: how accurate is the U-Th age of the last interglacial period? Earth Planet. Sci. Lett. 106, 169–180.
Harmon, R.S., Mitterer, R.M., Kriausakul, N., Land, L.S., Schwarcz, H.P., Garrett, P., Larson, G.J., Vacher, H.L., Rowe, M., 1983. U-series and amino-acid racemization geochronology of Bermuda: implications for eustatic sea-level fluctuation over the past 250,000 years. Palaeogeogr. Palaeoclimatol. Palaeoecol. 44, 41–70.
Henry, L.A., 1978a. Port Maria: Geological Sheet 21. Mines and Geology Division, Jamaica Ministry of Mining and Natural Resources scale1:50,000.
Henry, L.A., 1978b. Ocho Rios: Geological Sheet 18. Mines and Geology Division, Jamaica Ministry of Mining and Natural Resources scale1:50,000.
Hill, R.T., 1895. Notes on the geology of the Island of Cuba, based on a reconnaissance made for Alexander Agassiz. Bull. Mus. Comp. Zoology 16, 243–288.
Horsfield, W.T., 1975. Quaternary vertical movements in the greater Antilles. Geol. Soc. Am. Bull. 86, 933–938.
Kopp, R.E., Simons, F.J., Mitrovica, J.X., Maloof, A.C., Oppenheimer, M., 2009. Probabilistic assessment of sea level during the last interglacial stage. Nature 462, 863–868.
Lambeck, K., Purcell, A., Dutton, A., 2012. The anatomy of interglacial sea levels: the relationship between sea levels and ice volumes during the Last Interglacial. Earth Planet. Sci. Lett. 315–316, 4–11.
Ludwig, K.R., 2001. Users Manual for Isoplot/Ex, Rev. 2.49. Berkeley Geochronology Center, Berkeley, California, p. 55. Special Publication No. 1a.
Ludwig, K.R., Paces, J.B., 2002. Uranium-series dating of pedogenic silica and carbonate, Crater Flat, Nevada. Geochimica Cosmochimica Acta 66, 487–506.
Ludwig, K.R., Wallace, A.R., Simmons, K.R., 1985. The Schwartzwalder uranium deposit, II: age of uranium mineralization and Pb-isotope constraints on genesis. Econ. Geol. 80, 1858–1871.
Ludwig, K.R., Simmons, K.R., Szabo, B.J., Winograd, I.J., Landwehr, J.M., Riggs, A.C., Hoffman, R.J., 1992. Mass-spectrometric ^{230}Th-^{234}U-^{238}U dating of the Devils Hole calcite vein. Science 258, 284–287.
Ludwig, K.R., Muhs, D.R., Simmons, K.R., Halley, R.B., Shinn, E.A., 1996. Sea level records at ~80 ka from tectonically stable platforms: Florida and Bermuda. Geology 24, 211–214.
Mann, P., 2007. Global catalogue, classification and tectonic origins of restraining- and releasing bends on active and ancient strike-slip fault systems. Geol. Soc. Lond. Special Publ. 290, 13–142.
Mann, P., Taylor, F.W., Edwards, R.L., Ku, T.-L., 1995. Actively evolving microplate formation by oblique collision and sideways motion along strike-slip faults: an example from the northeastern Caribbean plate margin. Tectonophysics 246, 1–69.
Mann, P., Calais, E., Ruegg, J.-C., DeMets, C., Jansma, P.E., Mattioli, G.S., 2002. Oblique collision in the northeastern Caribbean from GPS measurements and geological

observations. Tectonics 21 (6). https://doi.org/10.1029/2001TC001304.
Martin, L., Suguio, K., Flexor, J.-M., 1988. Hauts niveaux marins Pleistocenes du littoral Bresilien. Palaeogeogr. Palaeoclimatol. Palaeoecol. 68, 231–239.
Martinson, D.G., Pisias, N.G., Hays, J.D., Imbrie, J., Moore Jr., T.C., Shackleton, N.J., 1987. Age dating and the orbital theory of the ice ages: Development of a high-resolution 0 to 300,000-year chronostratigraphy. Quat. Res. 27, 1–29.
Meinzer, O.E., 1933. Geological reconnaissance adjacent to Guantanamo bay, Cuba. J. Wash. Acad. Sci. 23, 246–260.
Mesolella, K.J., Matthews, R.K., Broecker, W.S., Thurber, D.L., 1969. The astronomical theory of climatic change: Barbados data. J. Geol. 77, 250–274.
Milne, G.A., Mitrovica, J.X., 2008. Searching for eustasy in deglacial sea-level histories. Quat. Sci. Rev. 27, 2292–2302.
Moore, W.S., Somayajulu, B.L.K., 1974. Age determinations of fossil corals using ^{230}Th/^{234}Th and ^{230}Th/^{227}Th. J. Geophys. Res. 79, 5065–5068.
Muhs, D.R., Simmons, K.R., 2017. Taphonomic problems in reconstructing sea-level history from the late Quaternary marine terraces of Barbados. Quat. Res. 88, 409–429.
Muhs, D.R., Simmons, K.R., Steinke, B., 2002a. Timing and warmth of the last interglacial period: new U-series evidence from Hawaii and Bermuda and a new fossil compilation for North America. Quat. Sci. Rev. 21, 1355–1383.
Muhs, D.R., Simmons, K.R., Kennedy, G.L., Rockwell, T.K., 2002b. The last interglacial period on the Pacific Coast of North America: timing and paleoclimate. Geol. Soc. Am. Bull. 114, 569–592.
Muhs, D.R., Simmons, K.R., Schumann, R.R., Halley, R.B., 2011. Sea-level history of the past two interglacial periods: new evidence from U-series dating of reef corals from south Florida. Quat. Sci. Rev. 30, 570–590.
Muhs, D.R., Pandolfi, J.M., Simmons, K.R., Schumann, R.R., 2012a. Sea-level history of past interglacial periods from uranium-series dating of corals, Curaçao, Leeward Antilles islands. Quat. Res. 78, 157–169.
Muhs, D.R., Simmons, K.R., Schumann, R.R., Groves, L.T., Mitrovica, J.X., Laurel, D., 2012b. Sea-level history during the Last Interglacial complex on San Nicolas Island, California: implications for glacial isostatic adjustment processes, paleozoogeography and tectonics. Quat. Sci. Rev. 37, 1–25.
Muhs, D.R., Meco, J., Simmons, K.R., 2014a. Uranium-series ages of corals, sea level history, and palaeozoogeography, Canary Islands, Spain: an exploratory study for two Quaternary interglacial periods. Palaeogeogr. Palaeoclimatol. Palaeoecol. 394, 99–118.
Muhs, D.R., Simmons, K.R., Schumann, R.R., Groves, L.T., DeVogel, S.B., Minor, S.A., Laurel, D., 2014b. Coastal tectonics on the eastern margin of the Pacific rim: late Quaternary sea-level history and uplift rates, Channel Islands National Park, California, USA. Quat. Sci. Rev. 105, 209–238.
Murray-Wallace, C.V., Woodroffe, C.D., 2014. Quaternary Sea Level Changes: a Global Perspective. Cambridge University Press, Cambridge, p. 484.
O'Leary, M.J., Hearty, P.J., Thompson, W.G., Raymo, M.E., Mitrovica, J.X., Webster, J.M., 2013. Ice sheet collapse following a prolonged period of stable sea level during the last interglacial. Nat. Geosci. 6, 796–800.
Otto-Bliesner, B.L., Marshall, S.J., Overpeck, J.T., Miller, G.H., Hu, A., CAPE last interglacial project members, 2006. Simulating Arctic climate warmth and icefield retreat in the last interglaciation. Science 311, 1751–1753.
Overpeck, J.T., Otto-Bliesner, B.L., Miller, G.H., Muhs, D.R., Alley, R.B., Kiehl, J.T., 2006. Paleoclimatic evidence for future ice-sheet instability and rapid sea-level rise. Science 311, 1747–1750.
Pandolfi, J.M., 2007. A new, extinct Pleistocene reef coral from the *Montastraea* "*annularis*" species complex. J. Paleontology 81, 472–482.
Pandolfi, J.M., Jackson, J.B.C., Geister, J., 2001. Geologically sudden extinction of two widespread late Pleistocene Caribbean reef corals. In: Jackson, J.B.C., Lidgard, S., McKinney, F.K. (Eds.), Evolutionary Patterns: Growth, Form, and Tempo in the Fossil Record. University of Chicago Press, Chicago, pp. 120–158.
Pindell, J.L., Kennan, L., 2009. Tectonic evolution of the Gulf of Mexico, Caribbean and northern South America in the mantle reference frame: an update. Geol. Soc. Lond. Special Publ. 328, 1–55.
Portell, R.W., McCleskey, T., Toomey, J.K., 2008. Fossil invertebrates of the U.S. Naval Station Guantanamo Bay, Cuba, Part 1, Pleistocene Marine mollusca. Division of Invertebrate Paleontology, Florida Museum of Natural History, 32 pp.
Portell, R.W., Klose, W., McCleskey, T., Toomey, J.K., 2009. Fossil invertebrates of the U.S. Naval Station Guantanamo Bay, Cuba, Part 2, Pleistocene Corals. Division of Invertebrate Paleontology, Florida Museum of Natural History, 28 pp.
Potter, E.-K., Lambeck, K., 2003. Reconciliation of sea-level observations in the western North Atlantic during the last glacial cycle. Earth Planet. Sci. Lett. 217, 171–181.
Prentice, C.S., Mann, P., Crone, A.J., Gold, R.D., Hudnut, K.W., Briggs, R.W., Koehler, R.D., Jean, P., 2010. Seismic hazard of the Enriquillo-Plantain Garden fault in Haiti inferred from palaeoseismology. Nat. Geosci. 3, 789–793.
Rojas-Agramonte, Y., Neubauer, F., Handler, R., Garcia-Delgado, D.E., Friedl, G., Delgado-Damas, R., 2005. Variation of palaeostress patterns along the Oriente transform wrench corridor, Cuba: significance for Neogene-Quaternary tectonics of the Caribbean realm. Tectonophysics 396, 161–180.
Schellmann, G., Radtke, U., 2004. A revised morpho- and chronostratigraphy of the Late and Middle Pleistocene coral reef terraces on southern Barbados (West Indies). Earth-Science Rev. 64, 157–187.
Shinn, E.A., Lidz, B.H., Kindinger, J.L., Hudson, J.H., Halley, R.B., 1989. Reefs of Florida and the Dry Tortugas: a Guide to the Modern Carbonate Environments of the Florida Keys and the Dry Tortugas. U.S. Geological Survey, St. Petersburg, Florida, p. 53.
Smith, D.A., Small, H.J., 1999. The CARIB97 high-resolution geoid height model for the Caribbean Sea. J. Geodesy 73, 1–9.
Speed, R.C., Cheng, H., 2004. Evolution of marine terraces and sea level in the last interglacial, Cave Hill, Barbados. Geol. Soc. Am. Bull. 116, 219–232.
Stein, M., Wasserburg, G.J., Aharon, P., Chen, J.H., Zhu, Z.R., Bloom, A., Chappell, J., 1993. TIMS U-series dating and stable isotopes of the last interglacial event in Papua New Guinea. Geochimica Cosmochimica Acta 57, 2541–2554.
Stirling, C.H., Esat, T.M., Lambeck, K., McCulloch, M.T., 1998. Timing and duration of the Last Interglacial: evidence for a restricted interval of widespread coral reef growth. Earth Planet. Sci. Lett. 160, 745–762.
Szabo, B.J., 1979. ^{230}Th, ^{231}Pa, and open system dating of fossil corals and shells. J. Geophys. Res. 84, 4927–4930.
Szabo, B.J., Ward, W.C., Weidie, A.E., Brady, M.J., 1978. Age and magnitude of the late Pleistocene sea-level rise on the eastern Yucatan Peninsula. Geology 6, 713–715.
Taber, S., 1934. Sierra Maestra of Cuba, part of the northern rim of the Bartlett Trough. Geol. Soc. Am. Bull. 45, 567–620.
Taggart, B.E., Joyce, J., 1990. Radiometrically dated marine terraces on northwestern Puerto Rico. In: Larue, D.K., Draper, G. (Eds.), Transactions of the 12th Caribbean Geological Conference. Miami Geological Society, pp. 248–258.
Tamisiea, M.E., Mitrovica, J.X., 2011. The moving boundaries of sea level change: understanding the origins of geographic variability. Oceanography 24, 24–39.
Taylor, F.W., Mann, P., 1991. Late Quaternary folding of coral reef terraces, Barbados. Geology 19, 103–106.
Thompson, W.G., Goldstein, S.L., 2005. Open-system coral ages reveal persistent suborbital sea-level cycles. Science 308, 401–404.
Thompson, W.G., Spiegelman, M.W., Goldstein, S.L., Speed, R.C., 2003. An open-system model for U-series age determinations of fossil corals. Earth Planet. Sci. Lett. 210, 365–381.
Thompson, W.G., Curran, H.A., Wilson, M.A., White, B., 2011. Sea-level oscillations during the last interglacial highstand recorded by Bahamas corals. Nat. Geosci. 4, 684–687.
Toscano, M.A., Rodriguez, E., Lundberg, J., 1999. Geologic investigation of the late Pleistocene Jaimanitas Formation: Science and society in Castro's Cuba. In: Curran, H.A., Mylroie, J.E. (Eds.), Proceedings of the 9th Symposium on the Geology of the Bahamas and Other Carbonate Regions. Bahamian Field Station, Ltd., San Salvador, Bahamas, pp. 125–142.
Toscano, M.A., Macintyre, I.G., Lundberg, J., 2012. Last interglacial reef limestones, northeastern St. Croix, US Virgin Islands—evidence of tectonic tilting and subsidence since MIS 5.5. Coral Reefs 31, 27–38.
Vacher, H.L., Rowe, M.P., 1997. Geology and hydrogeology of Bermuda. In: Vacher, H.L., Quinn, T.M. (Eds.), Geology and Hydrology of Carbonate Islands. Developments in Sedimentology, vol. 54. Elsevier, Amsterdam, pp. 35–90.
Vaughn, T.W., 1919. Fossil corals from Central America, Cuba, and Porto Rico, with an account of the American Tertiary, Pleistocene, and Recent coral reefs. U. S. Natl. Mus. Bull. 103, 189–524.
Veeh, H.H., 1966. ^{230}Th/^{238}U and ^{234}U/^{238}U ages of Pleistocene high sea-level stand. J. Geophys. Res. 71, 3379–3386.
Wehmiller, J.F., Simmons, K.R., Cheng, H., Edwards, R.L., Martin-McNaughton, J., York, L.L., Krantz, D.E., Shen, C.-C., 2004. Uranium-series coral ages from the U.S Atlantic Coastal Plain—the "80 ka problem" revisited. Quat. Int. 120, 3–14.
White, B., Curran, H.A., Wilson, M.A., 1998. Bahamian coral reefs yield evidence of a brief sea-level lowstand during the last interglacial. Carbonates Evaporites 13, 10–22.
Wilson, M.A., Curran, H.A., White, B., 1998. Paleontological evidence of a brief global sea-level event during the last interglacial. Lethaia 31, 241–250.
Winter, A., Paul, A., Nyberg, J., Oba, T., Lundberg, J., Schrag, D., Taggart, B., 2003. Orbital control of low-latitude seasonality during the Eemian. Geophys. Res. Lett. 30, 1163,. https://doi.org/10.1029/2002GL016275.
Woodring, W.P., Brown, J.S., Burbank, W.S., 1924. Geology of the Republic of Haiti. Haiti Department of Public Works, Port-au-Prince, p. 631.
Woodroffe, C.D., Stoddart, D.R., Harmon, R.S., Spencer, T., 1983. Coastal morphology and late Quaternary history, Cayman Islands, West Indies. Quat. Res. 19, 64–84.